

Coregulation of nitrous oxide emissions by nitrogen and temperature in China's third largest freshwater lake (Lake Taihu)

Qitao Xiao,¹ Xiaofeng Xu,^{2,3} Mi Zhang,⁴ Hongtao Duan ,^{1*} Zhenghua Hu,⁴ Wei Wang,⁴ Wei Xiao,⁴ Xuhui Lee^{4,5*}

¹Key Laboratory of Watershed Geographic Sciences, Nanjing Institute of Geography and Limnology, Chinese Academy of Sciences, Nanjing, China

²Biology Department, San Diego State University, San Diego, California

³Northeast Institute of Geography and Agroecology, Chinese Academy of Sciences, Changchun, China

⁴Yale-NUIST Center on Atmospheric Environment, International Joint Laboratory on Climate and Environment Change, Nanjing University of Information Science and Technology, Nanjing, China

⁵School of Forestry and Environmental Studies, Yale University, New Haven, Connecticut

Abstract

Nitrous oxide (N₂O) is a potent greenhouse gas and contributes to the loss of stratospheric ozone. However, the role of inland waterbodies in the dynamics of atmospheric N₂O is poorly understood. We investigated N₂O fluxes and their controlling factors in Lake Taihu, a large and shallow (2400 km², 1.9 m depth) eutrophic lake in eastern China. Long-term measurements (2011–2016) revealed spatial and temporal variations in the lake surface N₂O fluxes. The mean N₂O flux from the lake was 3.5 ± 1.8 (mean ± SD) μmol m⁻² d⁻¹, with an annual N₂O budget of 134.4 ± 69.8 Mg (10⁶ g) yr⁻¹. The highest N₂O fluxes occurred in the eutrophic zone with significant anthropogenic N inputs, and the lowest fluxes occurred in the noneutrophic zone with no external N inflow. A seasonal pattern in N₂O fluxes was observed only in the noneutrophic zone and was strongly correlated with water temperature. No seasonality in the N₂O fluxes was observed in the eutrophic zone with high N concentrations in the water, indicating that N concentrations play a dominant role in regulating N₂O fluxes compared to water temperature. The average N₂O emission factor in Lake Taihu was 0.18%, with temporal and spatial variations negatively associated with N concentration but positively associated with the mass ratio of dissolved organic carbon to dissolved inorganic nitrogen. Our results suggest that anthropogenic activities strongly affect N₂O fluxes in freshwater lakes.

Nitrous oxide (N₂O) is a potent greenhouse gas with a radiative forcing of 0.17 W m⁻², ranking third among the long-lived greenhouse gases in the atmosphere (IPCC 2013). At the same time, N₂O plays a major role in ozone depletion in the stratosphere (Ravishankara et al. 2009). There has been a steady increase in atmospheric N₂O at a rate of 0.7–0.8 ppb yr⁻¹ over the past three decades (Davidson 2009; Saikawa et al. 2014). The growing atmospheric concentration of N₂O and its biological sources from the biosphere have received considerable attention, and a number of studies has been carried out to investigate the terrestrial sources of N₂O, such as natural soils (Chapuis-Lardy et al. 2007; Xu et al. 2008), synthetic fertilizers (Davidson 2009; Saikawa et al. 2014; Griffis et al. 2017), and wastewater treatment (Kampschreur et al. 2009; Foley et al. 2010).

Inland freshwater systems remain understudied in terms of their N₂O budget due to their high heterogeneity (Ivens et al. 2011; Borges et al. 2015). Inland waters can receive large N loadings from human activities, depending particularly on farming practices (Seitzinger and Kroeze 1998; Ivens et al. 2011; McCrackin and Elser 2011; Borges et al. 2018). N₂O is an intermediate product of denitrification, the microbial reduction of nitrate (NO₃⁻-N) to nitrite (NO₂⁻-N), nitric oxide (NO), N₂O, and N₂, and is a byproduct of nitrification, the microbial oxidation of ammonium (NH₄⁺-N) to NO₂⁻-N and NO₃⁻-N. These microbial processes can significantly occur in lakes (Seitzinger et al. 2006), making lakes a strong source of atmospheric N₂O. The relatively long-residence time of lakes makes these waterbodies more effective than rivers in N removal and associated N₂O production (Mulholland et al. 2008; Harrison et al. 2009). Thus, a more accurate estimation of N₂O emissions from inland lakes is fundamental for quantifying an N₂O budget at a regional scale.

*Correspondence: htduan@niglas.ac.cn or xuhui.lee@yale.edu

Additional Supporting Information may be found in the online version of this article.

Previous studies on N₂O dynamics in freshwater lakes largely focus on boreal lakes (Mengis et al. 1996; Huttunen et al. 2003; Miettinen et al. 2015; Soued et al. 2016; Klaus et al. 2017). Also, lake eutrophication and the associated decrease in the biomass of submerged macrophytes are widespread (Sinha et al. 2017; Zhang et al. 2017), but the effects of eutrophication and submerged macrophyte coverage on N₂O fluxes remain uncertain. An increasing trend of N₂O emissions from oligotrophic to eutrophic lakes was found as a result of increasing external N loading (Mengis et al. 1997; Huttunen et al. 2003; Wang et al. 2007; Whitfield et al. 2011). This finding is in contrast to an ecosystem-scale experiment which reported a neutral response of N₂O fluxes to N enrichment in unproductive boreal lakes (Klaus et al. 2017). It has been reported that submerged macrophytes influenced lake N cycling and were significantly correlated with variability in N₂O fluxes (Davidson et al. 2015; Zhu et al. 2015). However, a number of studies have reported that submerged macrophytes do not enhance lake N removal and the associated N₂O production (Liu et al. 2017; Yao et al. 2017). Considering these contrasting results, large uncertainties remain on how eutrophication and macrophytes affect N₂O emissions from freshwater lakes.

The Intergovernmental Panel on Climate Change (IPCC) guidelines on national greenhouse gas inventories recognize that a fraction of N is converted to N₂O from N fertilizer leaching and runoff from agriculture soils. Such substance-based N₂O fluxes are defined as indirect emissions. The indirect N₂O emission factor (EF) allows for the estimation of N₂O emissions based on information of the external N inputs or background N concentrations in a system (De Klein et al. 2006). Global and regional N₂O emissions from a waterbody can be approximated by multiplying the nitrogen fertilizer input or relevant anthropogenic N loading with a predetermined EF (De Klein et al. 2006; Ivens et al. 2011; McCrackin and Elser 2011; Hu et al. 2016; Hama-Aziz et al. 2017; Fu et al. 2018). However, it should be noted that the unitless EF value can vary by an order of magnitude (Beaulieu et al. 2011; McCrackin and Elser 2011; Turner et al. 2015; Hama-Aziz et al. 2017). For example, the current default EF for rivers is 0.0025 (De Klein et al. 2006), but studies suggest that this value can be either underestimated (Beaulieu et al. 2011; Yu et al. 2013; Turner et al. 2015; Fu et al. 2018) or overestimated (Outram and Hiscock 2012; Hama-Aziz et al. 2017). In general, the EF estimates for lakes are poorly understood due to the limited number of studies in these complex ecosystems (McCrackin and Elser 2011; Outram and Hiscock 2012). More EF measurements are needed to better estimate indirect N₂O budgets (McCrackin and Elser 2011).

In this study, we report the results of field experiments on N₂O fluxes from Lake Taihu, a typical subtropical eutrophic lake in the Yangtze River Delta, China. The lake has a complex river network with 117 rivers or channels draining into the lake (Xu et al. 2010). The northern and western portions of the lake experience severe eutrophication due to pollution discharge by

inflow rivers (Qin et al. 2007). Submerged vegetation dominates much of the eastern portion of the lake, with an average macrophyte biomass of 3.8 kg m⁻² (Qin et al. 2007; Luo et al. 2016). The effects of anthropogenic N inputs and the presence of macrophytes on the lake water quality have been well documented (Qin et al. 2007; Duan et al. 2009; Xu et al. 2010); however, their roles in N₂O emissions remain poorly investigated.

The objectives of this study are as follows: (1) to characterize the spatiotemporal variations in N₂O fluxes across the entire Lake Taihu; (2) to investigate the control of biological, chemical, and physical processes on the N₂O fluxes; and (3) to quantify the N₂O contribution from Lake Taihu to the national N₂O budget.

Materials and methods

Study area

Measurements were made in Lake Taihu (30°05′–32°08′N, 119°08′–121°55′E) in eastern China. Lake Taihu is the third largest freshwater lake in China, with a surface area of 2400 km² and a mean depth of 1.9 m. The lake catchment covers approximately 36,500 km², with a complicated river network surrounded by several large cities. Inflow comes from the northern and western sides of the lake, and outflow occurs on the eastern side of the lake (Fig. 1). The local climate is characterized by high-water temperatures (monthly mean: 31°C) and rain (monthly mean: 170 mm) in the summer and low temperatures and rain in the winter (monthly mean water temperature: 3.9°C; monthly mean rain: 60 mm; Xu et al. 2010; Xiao et al. 2017). The annual precipitation is approximately 1100 mm (Lee et al. 2014; Wang et al. 2014). The anthropogenic N inputs through inflow were 2–4 times higher than the N loss via river outflow (Supporting Information Table S1 and Fig. S1). High concentrations of dissolved organic carbon (DOC) occur in the eutrophic zone due to anthropogenic inputs via river discharge and in the macrophyte-dominated zone due to carbon accumulation via primary production (Lee et al. 2014). Major pollutant sources, including industrial activities, domestic sewage, and agricultural fertilizers, are present in the catchment (Qin et al. 2007; Duan et al. 2009).

We divided Lake Taihu into three zones according to the geographic differences in vegetation and nutrient concentrations (Fig. 1). Zone 1 is the most eutrophic part of the lake, with elevated nutrient loads from river inputs, including the hypereutrophic northwest zone and Meiliang Bay. Zone 3 is the main outlet of the lake and is characterized by dense submerged vegetation (mainly *Hydrilla verticillata* and *Potamogeton malaianus*). Zone 2 has lower eutrophication and represents a transitional area (Fig. 1). This is seen in the typical mean dissolved oxygen (DO) concentrations of 6.94 mg L⁻¹, 10.03 mg L⁻¹, and 10.72 mg L⁻¹ for zone 1, zone 2, and zone 3, respectively (Xiao et al. 2017), and in the average macrophyte coverage of 3.8 kg m⁻² in zone 3 and close to zero in the other zones (Qin et al. 2007; Luo et al. 2016). The spatial contrast in the total

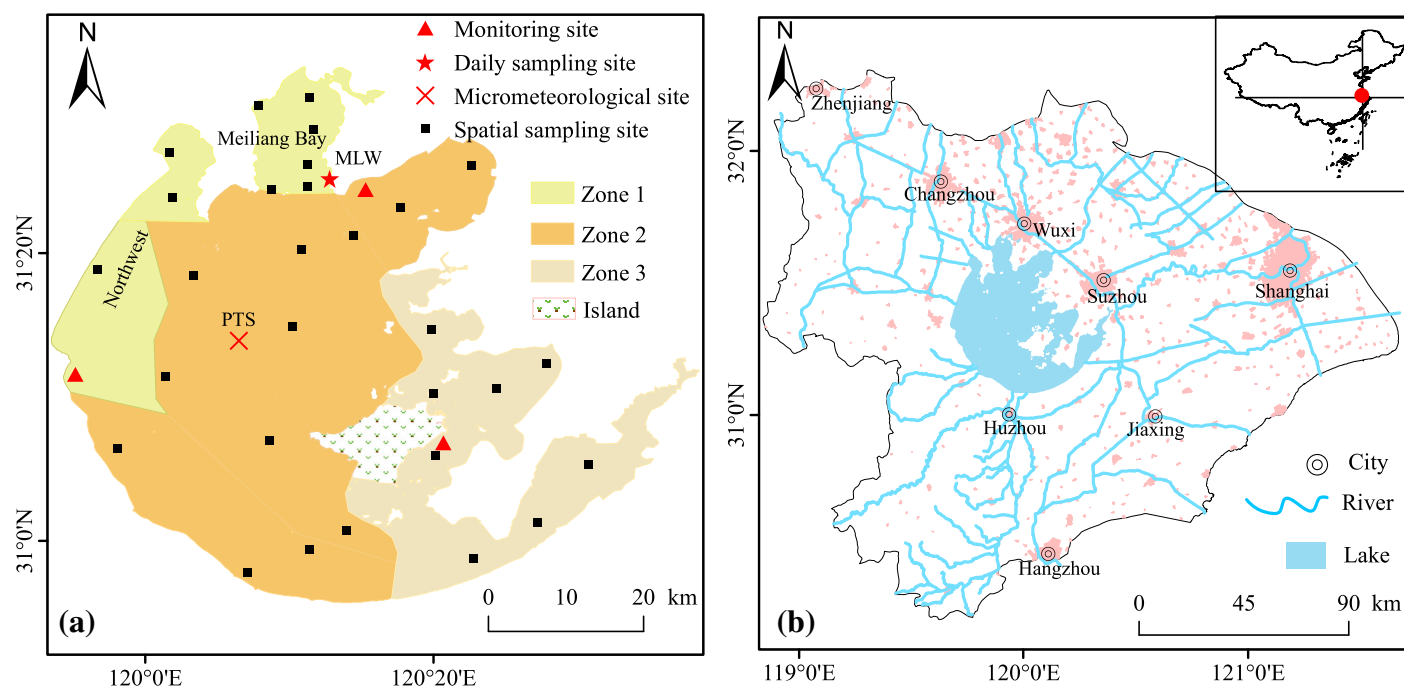


Fig. 1. Geographic location of Lake Taihu and the sampling sites; **(a)** The location of the spatial sampling sites and three biological zones at Lake Taihu: black squares, spatial sampling sites; red star, daily sampling site; red cross, PTS (Pingtaishan) lake micrometeorological site; red triangles, in situ high-frequency measurements by the China National Environmental Monitoring Center (<http://www.zhb.gov.cn/hjzl/shj/dbszdczb/>). Zone 1: eutrophic zone, including the Northwest Zone and Meiliang Bay; Zone 2: transition zone; Zone 3: Submerged macrophyte zone. **(b)** Lake Taihu watershed and surrounding rivers. Water flows from the north and west to the east and south. [Color figure can be viewed at wileyonlinelibrary.com]

nitrogen (TN) concentrations of zone 1, zone 2, and zone 3, with values of 2.58 mg L⁻¹, 1.89 mg L⁻¹, and 1.07 mg L⁻¹, respectively (Xiao et al. 2017), also supports this finding.

N₂O lake surveys

Lake water samples were collected in 300 mL glass bottles to analyze the spatial-temporal variability in N₂O concentrations. The sampling procedures have previously been reported in detail (Xiao et al. 2017). Briefly, bubble-free lake water was collected at the desired depth below the lake surface using a custom-made sampler sealed with a rubber cork. The cork was removed from the opening by remote control when the sampler reached the desired depth, allowing water to enter the sampler. The water was then poured quickly into a 300 mL glass bottle, and the bottle was immediately capped without headspace using a butyl rubber stopper and sealed with a sealing membrane. Both the glass bottle and sampler were washed with local bubble-free lake water before collection.

Surface lake water samples were collected daily at a depth of 20 cm at midday from 01 August 2011 to 31 December 2016 at a fixed sample site 200 m from the shore in Meiliang Bay at the northern part of the lake (the MLW (Meiliangwan) site, 31°24'N, 120°13'E, Fig. 1). A total of 1980 water samples were collected at the MLW site to explore the temporal variation in N₂O. Diel sampling was also conducted at the MLW site to investigate diel variations in the N₂O fluxes. Surface-water

samples were collected every 3 h for three consecutive days in each month from August 2011 to July 2013. Water samples were also collected at depths of 20 cm, 50 cm, 100 cm, and 150 cm at 00:00 h and 12:00 h every day during diel sampling to explore the vertical profiles of dissolved N₂O concentrations.

Whole-lake surveys were conducted seasonally from 2012 to 2016 in mid-February, mid-May, mid-August, and mid-November. In each whole-lake survey, surface-water samples were collected at a depth of 20 cm from each of the 29 sampling locations (Fig. 1). Each of these included 9 sampling sites in zone 1, 12 in zone 2, and 8 in zone 3. The sampling sites in each zone were evenly spatially distributed. Over the 5-yr sampling period, a total of 580 water samples were collected from zone 1 ($n = 180$), zone 2 ($n = 240$) and zone 3 ($n = 160$) to explore the spatial variability in N₂O concentrations and fluxes. Each whole-lake survey was completed in two consecutive days to reduce the biases caused by day-to-day variations and by one person to reduce systems bias.

Dissolved N₂O concentrations in the collected water samples were analyzed using the headspace equilibration method (Mengis et al. 1996; Davidson et al. 2015). Ultrahigh purity N₂ gas (99.999%) was injected into the glass bottle to create a 100-mL headspace. The glass bottle was then shaken vigorously for 5 min to allow the dissolved N₂O gas to reach equilibrium within the headspace. A small air sample (20 mL) was drawn from the headspace using a syringe with a three-way stopcock and was injected into a gas chromatograph (Model

Agilent GC7890B, Agilent, California, U.S.A.) equipped with an electronic capture detector for N₂O detection.

N₂O flux calculation

The N₂O fluxes (F_n , $\mu\text{mol m}^{-2} \text{d}^{-1}$; a positive value indicates N₂O emission from the water to atmosphere) at the lake–air interface were calculated using the transfer coefficient method based on the bulk diffusion model (Eq. 1; Cole and Caraco 1998):

$$F_n = k \times (C_w - C_{\text{eq}}) \quad (1)$$

where C_w is the dissolved N₂O concentration ($\mu\text{mol m}^{-3}$) in the surface water (top 20 cm), as measured by gas chromatography, and C_{eq} is the N₂O concentration in water in equilibrium with the atmosphere at the in situ temperature. k is the gas transfer coefficient (m d^{-1}) and was normalized to a Schmidt number of 600 (Eq. 2):

$$k/k_{600} = (S_c/S_{c600})^{-n} \quad (2)$$

where S_c is the Schmidt number of a given gas at a given temperature and water density, S_{c600} is the Schmidt number 600 at a temperature of 20°C, n is a constant determined by measured wind speed, and k_{600} is the gas transfer coefficient adjusted to Schmidt number 600 calculated by wind speed (Cole and Caraco 1998):

$$k_{600} = 2.07 + 0.215 \times U_{10}^{1.7} \quad (3)$$

where U_{10} is the wind speed at a 10-m height. The hourly wind speed measured at the PTS site, a micrometeorological site located in the center of Lake Taihu (Fig. 1; Lee et al. 2014), was used to calculate the gas transfer coefficient. Although there are a number of formulations considering both wind shear and waterside convection reported for the k_{600} calculation (e.g., MacIntyre et al. 2010), our previous study confirmed that the gas transfer coefficient in the large lake was mostly driven by wind speed (Xiao et al. 2017), which is consistent with Read et al. (2012). There were no significant differences between k values calculated by the wind-dependent model described by Cole and Caraco (1998) and those calculated by models considering both wind shear and waterside convection in the lake (Xiao et al. 2017).

N₂O emission factor calculation

EF was calculated with two different approaches (Outram and Hiscock 2012; Hama-Aziz et al. 2017). The first method, herein known as EF_a for the whole lake, was computed by dividing the annual N₂O fluxes from the lake by the total amount of N loading in 1 yr, following the IPCC approach for calculating national N₂O inventories. The second method, defined as EF_b, was calculated by using N₂O-N/NO₃⁻-N mass ratios (McCrackin and Elser 2011; Outram and Hiscock 2012;

Turner et al. 2015; Hama-Aziz et al. 2017; Fu et al. 2018). The EF_a was calculated for the whole lake, without information on the spatiotemporal variation in N processes. Most reported EFs for aquatic systems are computed with the second method (Outram and Hiscock 2012; Turner et al. 2015; Hama-Aziz et al. 2017).

Auxiliary data

Hourly micrometeorological measurements at the PTS site included wind speed, wind direction, water temperature, air temperature, relative humidity, and four-way net radiation components (Lee et al. 2014; Xiao et al. 2017). Triplicate water samples were collected at the micrometeorological site for N₂O measurements during every site visit. During each survey, the physical, biological, and chemical properties (water temperature, pH, specific conductance [Spc], oxidation reduction potential [ORP], and DO concentration) were measured in situ with a multiparameter probe (YSI 650MDS, YSI, Yellow Springs, Ohio, U.S.A.) at a depth of 20 cm to be consistent with the water sampling. The YSI parameters were calibrated before each survey to reduce the uncertainty. It should be noted that water temperature profile measurements were conducted hourly at the MLW site (Lee et al. 2014).

The concentrations of nutrients (TN, total phosphorus [TP], ammonium, nitrate, and nitrite), DOC, and chlorophyll *a* (Chl *a*) were analyzed at each of the 29 sampling locations during the whole-lake surveys. Surface-water samples were collected from each spatial sampling site using an organic glass hydrophore and stored in acid-washed plastic bottles. Samples were preserved in ice-chilled coolers and transported to the laboratory for filtration and measurements. The concentrations of TN and TP were measured using combined persulfate digestion (Ebina et al. 1983). Ammonium (NH₄⁺-N) was determined by the indophenol blue method with a spectrophotometer at 640 nm, and nitrate (NO₃⁻-N) and nitrite (NO₂⁻-N) were determined with the cadmium reduction method with a spectrophotometer at 543 nm (American Public Health Association 1995). The DOC concentrations were analyzed after filtration through precombusted 47 mm GF/F filters (porosity 0.7 μm) with a Shimadzu TOC-5000A analyzer (Duan et al. 2014). The Chl *a* was extracted with 90% hot ethanol and concentrations were determined spectrophotometrically at 665 nm and 750 nm using a Shimadzu spectrophotometer.

Data analysis

Simple linear regression and multilinear stepwise regression were carried out to find correlations between the environmental variables and N₂O fluxes. The zonal mean N₂O fluxes and environmental variables were used for temporal analysis. A zonal mean was calculated for each lake survey using all measurements within the corresponding zone. In total, there were 20 data sets for temporal correlation analysis. The flux of each lake zone was computed as the mean of all calculated fluxes in

the same zone; then, the whole-lake N₂O fluxes were computed as an area-weighted zonal flux.

A least significant difference post hoc test was conducted to examine the differences among measured variables using SPSS (version 18.0). Differences at the $p < 0.05$ level were deemed statistically significant.

Results

Environmental condition

There was no substantial spatial variation in water temperature across Lake Taihu (Xiao et al. 2017); the temperature variation was $< 0.6^\circ\text{C}$ between different zones (Wang et al. 2014). The water temperature also showed no vertical profile variation from the surface to the bottom of Lake Taihu (Supporting Information Fig. S2a,b), indicating that the lake was well mixed due to its shallow depth. There was a clear seasonality; the annual mean water temperature at a 20-cm depth was 17.9°C , with the highest water temperature in August (37.3°C) and the lowest in January (0.1°C). The annual mean wind speed was 4.5 m s^{-1} , with no significant spatial variation across the open water (Xiao et al. 2017).

Lake Taihu showed strong spatial variation in water chemistry (Table 1; Fig. 2). The highest concentrations of NH₄⁺-N (1.75 mg L^{-1}), NO₃⁻-N (1.24 mg L^{-1}), NO₂⁻-N (0.19 mg L^{-1}), TN (5.25 mg L^{-1}), and TP (0.29 mg L^{-1}) occurred in zone 1 and were associated with discharge from inflowing rivers. Zone 1 had significantly ($p < 0.05$) higher nutrient concentrations than zone 2 and zone 3. In contrast, the lowest DO and pH were generally found in zone 1 (Fig. 2), and there were no significant differences among the three zones ($p > 0.05$). The spatial variations of various forms of N were highly intercorrelated (Fig. 2); for example, the NO₂⁻-N concentration was highly correlated with NO₃⁻-N ($r = 0.88$, $p < 0.01$) and NH₄⁺-N ($r = 0.99$, $p < 0.01$) across the lake. The mean Chl *a* concentration in zone 1 ($35.74 \mu\text{g L}^{-1}$) was also significantly ($p < 0.05$) higher than that in zones 2 and 3.

Some environmental variables showed seasonal variations among the three zones (Fig. 3). The DO varied seasonally, with the peak occurring in winter (Fig. 3b). The seasonal variation in Chl *a* was consistent with water temperature (Fig. 3a,c),

with significantly ($p < 0.05$) higher concentrations in summer than in winter for the three zones. In contrast, NH₄⁺-N and NO₃⁻-N concentrations were higher in winter (Fig. 3d,e). It should be noted that zone 1 had the highest Chl *a* and nutrient concentrations over the study period.

Spatial and temporal variations in N₂O concentrations and fluxes

Sampling at different water depths at MLW from September 2011 to July 2013 indicated that, in general, dissolved N₂O concentrations were remarkably uniform on the vertical profiles (Supporting Information Fig. S2c,d). On the contrary, N₂O concentrations in the surface waters varied dramatically based on the total 20 whole-lake surveys from 2012 to 2016 (Supporting Information Fig. S3). Surface dissolved N₂O concentrations varied within wide ranges of $6.8\text{--}129.9 \text{ nmol L}^{-1}$ in spring, $6.0\text{--}91.6 \text{ nmol L}^{-1}$ in summer, $4.5\text{--}133.8 \text{ nmol L}^{-1}$ in autumn, and $5.9\text{--}99.7 \text{ nmol L}^{-1}$ in winter. The average seasonal N₂O concentrations in the lake were 15.5 nmol L^{-1} , 12.1 nmol L^{-1} , 14.8 nmol L^{-1} , and 17.4 nmol L^{-1} , in spring, summer, fall, and winter, respectively.

The N₂O fluxes showed large spatial variations across the lake (Figs. 4, 5). The N₂O fluxes in zone 1, with an annual mean value of $11.4 \mu\text{mol m}^{-2} \text{ d}^{-1}$, were significantly ($p < 0.01$) higher than those in zones 2 and 3 ($\sim 1.3 \mu\text{mol m}^{-2} \text{ d}^{-1}$), while there was no significant difference ($p = 0.87$) in these fluxes between zone 2 and zone 3. The spatial N₂O fluxes ranged between $0.9 \mu\text{mol m}^{-2} \text{ d}^{-1}$ and $58.7 \mu\text{mol m}^{-2} \text{ d}^{-1}$ in spring, $-0.1 \mu\text{mol m}^{-2} \text{ d}^{-1}$ and $62.5 \mu\text{mol m}^{-2} \text{ d}^{-1}$ in summer, $-1.5 \mu\text{mol m}^{-2} \text{ d}^{-1}$ and $55.6 \mu\text{mol m}^{-2} \text{ d}^{-1}$ in autumn, and $-1.7 \mu\text{mol m}^{-2} \text{ d}^{-1}$ and $39.1 \mu\text{mol m}^{-2} \text{ d}^{-1}$ in winter, showing nonsignificant ($p > 0.05$) differences among the seasons. The amplitude (maximum minus minimum) of the N₂O fluxes across the whole lake in summer ($62.6 \mu\text{mol m}^{-2} \text{ d}^{-1}$) was larger than that in winter ($40.8 \mu\text{mol m}^{-2} \text{ d}^{-1}$).

The N₂O fluxes at the water-air interface showed strong temporal variation over the whole lake (Fig. 5) and at the MLW site (Fig. 6). During whole-lake sampling, the highest N₂O flux was found in summer and the lowest in winter, but the differences between seasons were nonsignificant ($p > 0.05$)

Table 1. Annual mean nutrient concentration and Chl *a* concentration across three zones in Lake Taihu from 2012 to 2015.

Zone	Type	Statistics	NH ₄ ⁺ -N ($\mu\text{mol L}^{-1}$)	NO ₃ ⁻ -N ($\mu\text{mol L}^{-1}$)	NO ₂ ⁻ -N ($\mu\text{mol L}^{-1}$)	TN ($\mu\text{mol L}^{-1}$)	TP (mg L^{-1})	DOC (mg L^{-1})	Chl <i>a</i> ($\mu\text{g L}^{-1}$)	DOC : DIN
Zone 1	Eutrophic	Mean \pm SD	54 \pm 31	53 \pm 31	4.95 \pm 2.00	232 \pm 54	0.17 \pm 0.06	4.74 \pm 0.75	35.74 \pm 28.75	6.36 \pm 4.19
		Range	50–122	16–101	3.01–11.05	161–319	0.12–0.32	3.77–5.88	7.96–109.98	1.68–14.17
Zone 2	Transitional	Mean \pm SD	24 \pm 11	39 \pm 24	1.17 \pm 0.66	152 \pm 45	0.10 \pm 0.02	3.84 \pm 0.84	20.19 \pm 11.11	7.03 \pm 6.88
		Range	8–48	11–77	0.38–2.71	99–206	0.07–0.14	2.51–5.33	8.14–46.45	2.01–12.61
Zone 3	Macrophytes	Mean \pm SD	18 \pm 9	19 \pm 16	0.54 \pm 0.26	92 \pm 32	0.05 \pm 0.02	3.67 \pm 0.81	8.88 \pm 3.29	9.64 \pm 4.42
		Range	6–38	4–49	0.18–0.99	55–148	0.03–0.10	2.52–5.20	4.56–16.50	3.31–16.72

Chl *a*, chlorophyll *a* concentration; DOC, dissolved organic carbon; DOC : DIN, the mass ratio of DOC (mg L^{-1}) to DIN (dissolved inorganic nitrogen, mg L^{-1}); TN, total nitrogen concentration; TP, total phosphorus concentration.

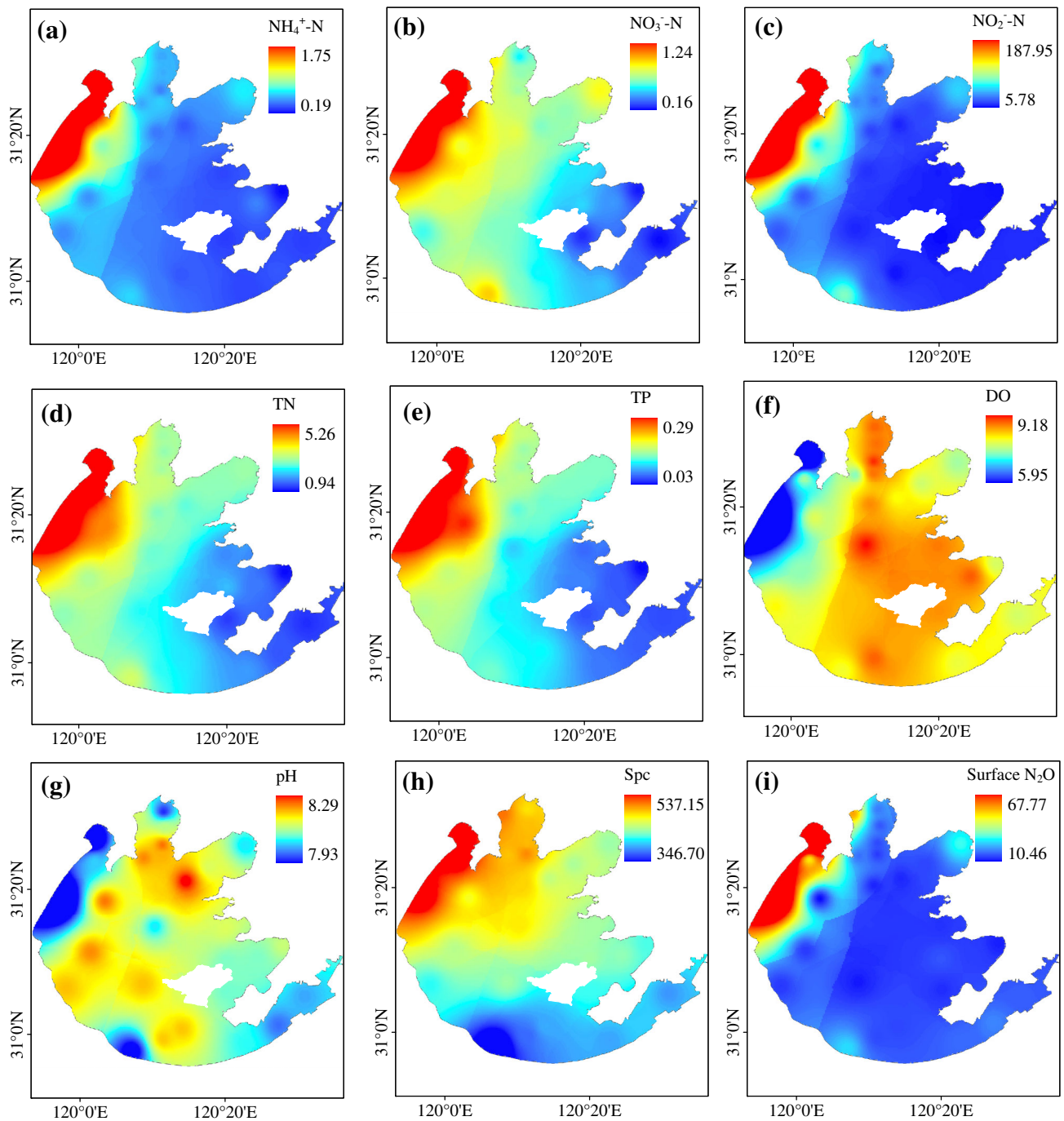


Fig. 2. Spatial variation in N loading, water quality indices, and dissolved N₂O concentration across Lake Taihu during the sampling period: (a) NH₄⁺-N (mg L⁻¹), (b) NO₃⁻-N (mg L⁻¹), (c) NO₂⁻-N (μg L⁻¹), (d) TN (mg L⁻¹), (e) TP (mg L⁻¹), (f) DO (mg L⁻¹), (g) pH, (h) specific conductance (Spc, μmS cm⁻¹), and (i) surface dissolved N₂O concentration (nmol L⁻¹). [Color figure can be viewed at wileyonlinelibrary.com]

due to high-temporal variability. From MLW daily sampling, the average winter (December, January, and February) flux was 0.4 μmol m⁻² d⁻¹, approximately 14 times lower than the summer (June, July, and August) flux (5.1 μmol m⁻² d⁻¹), with a statistically significant difference ($p < 0.01$). Approximately 30% of the sampled water at the MLW site was undersaturated in terms of N₂O, most often occurring in winter.

Multiple-year measurements showed a substantial interannual variability in the whole-lake N₂O fluxes. The largest N₂O fluxes occurred in 2012, with a mean value of 5.5 μmol m⁻² d⁻¹, and the lowest N₂O fluxes occurred in 2016, with a mean value of 1.1 μmol m⁻² d⁻¹. The most substantial interannual variability in N₂O fluxes was observed in zone 1, which showed a sharp decrease in annual fluxes from 18.1 μmol m⁻² d⁻¹ in 2012 to

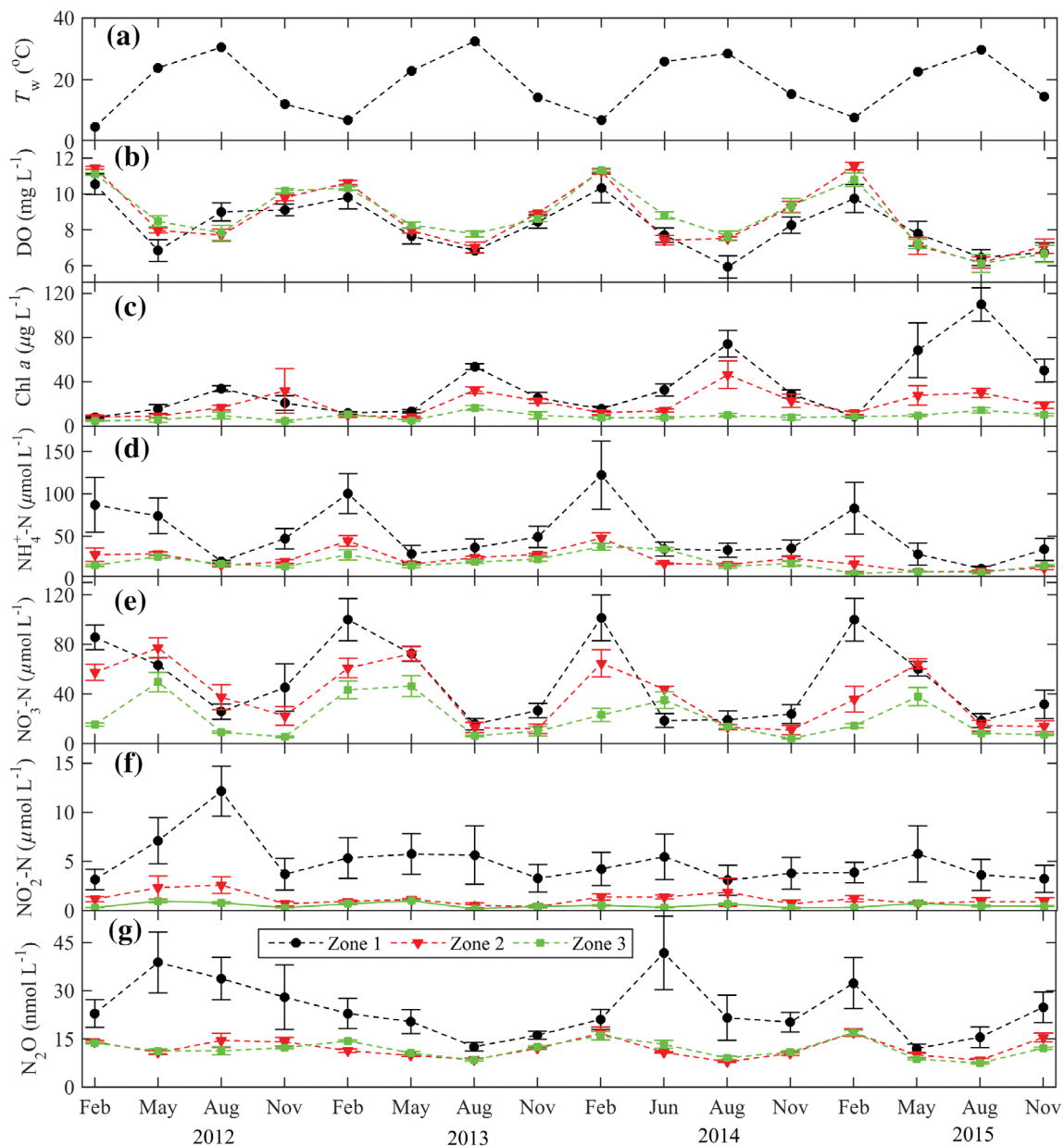


Fig. 3. Seasonal variation in (a) water temperature (T_w), (b) DO, (c) Chl *a* concentration, (d) NH_4^+ -N, (e) NO_3^- -N, (f) NO_2^- -N, and (g) surface dissolved N_2O concentration in the three zones. Note that the water temperature was the monthly mean value obtained from the MLW site (Lee et al. 2014). Error bars indicate one standard error. [Color figure can be viewed at wileyonlinelibrary.com]

$3.6 \mu\text{mol m}^{-2} \text{d}^{-1}$ in 2016 (Fig. 4; Table 2). The N_2O fluxes in zones 2 and 3 also showed substantial interannual variability (Table 2) and decreased from $2.4 \mu\text{mol m}^{-2} \text{d}^{-1}$ in 2012 to $0.4 \mu\text{mol m}^{-2} \text{d}^{-1}$ in 2016 (zone 2) and from $1.3 \mu\text{mol m}^{-2} \text{d}^{-1}$ in 2012 to $0.6 \mu\text{mol m}^{-2} \text{d}^{-1}$ in 2016 (zone 3). However, as a whole, these interannual variability trends were nonsignificant over the study period (zone 1: $p = 0.13$; zone 2: $p = 0.37$; zone 3: $p = 0.22$; whole lake: $p = 0.13$). The annual mean N_2O flux was $3.5 \pm 1.8 \mu\text{mol m}^{-2} \text{d}^{-1}$ based on long-term measurements (Table 2), with an annual N_2O budget of $134.4 \pm 69.8 \text{ Mg}$ (10^6 g) yr^{-1} .

Diurnal sampling showed statistically insignificant diel variations in N_2O fluxes (Supporting Information Fig. S4). In cold seasons, the hourly N_2O fluxes varied within relatively narrow ranges, showing nonsignificant ($p = 0.99$) differences between daytime fluxes and nighttime fluxes. In warm seasons, the hourly N_2O fluxes varied within wide ranges, for example, ranging between $5.5 \mu\text{mol m}^{-2} \text{d}^{-1}$ and $21.9 \mu\text{mol m}^{-2} \text{d}^{-1}$ in June 2012, also leading to nonsignificant ($p = 0.84$) differences between daytime fluxes and nighttime fluxes. Interestingly, the annual mean daytime flux ($2.9 \pm 0.2 \mu\text{mol m}^{-2} \text{d}^{-1}$) was the same as the annual mean nighttime flux ($2.9 \pm 0.1 \mu\text{mol m}^{-2} \text{d}^{-1}$,

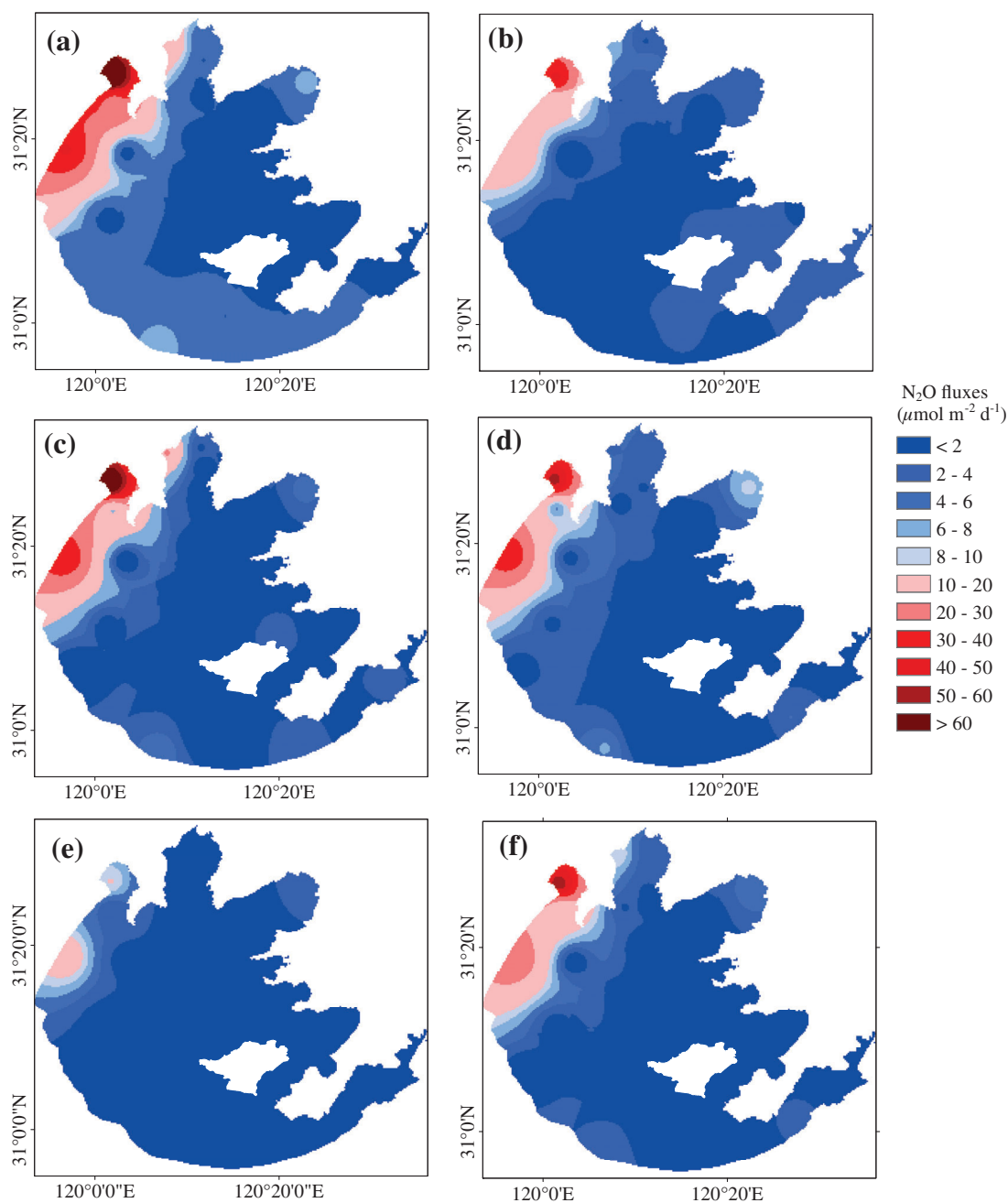


Fig. 4. Spatial variation in the annual mean N₂O fluxes during the sampling period: (a) 2012, (b) 2013, (c) 2014, (d) 2015, (e) 2016, and (f) mean value during 2012–2016. [Color figure can be viewed at wileyonlinelibrary.com]

Supporting Information Fig. S4) during the sampling period. Hence, we did not consider diel variations when computing N₂O budgets in the following sections.

Factors influencing N₂O fluxes

There were statistically significant linear correlations between the water temperature and N₂O fluxes for zone 2 ($r = 0.49$; $p = 0.028$), zone 3 ($r = 0.60$; $p = 0.005$), and the whole lake ($p = 0.015$). However, no significant correlation was found between the water temperature and N₂O fluxes

within zone 1 (Table 3). No relationship was found between the wind speed and whole-lake mean N₂O fluxes ($p = 0.80$). Daily sampling at MLW from August 2011 to December 2016 also confirmed the influence of water temperature on N₂O fluxes ($r = 0.34$, $p < 0.01$; Supporting Information Fig. S5).

The variabilities in N₂O fluxes were correlated with several environmental variables (Fig. 7; Table 4). Based on the continuous whole-lake survey over space and time across the nutrient gradient, the N₂O fluxes were positively correlated with NO₂⁻-N ($r = 0.68$, $p < 0.01$, $n = 460$), NO₃⁻-N ($r = 0.30$,

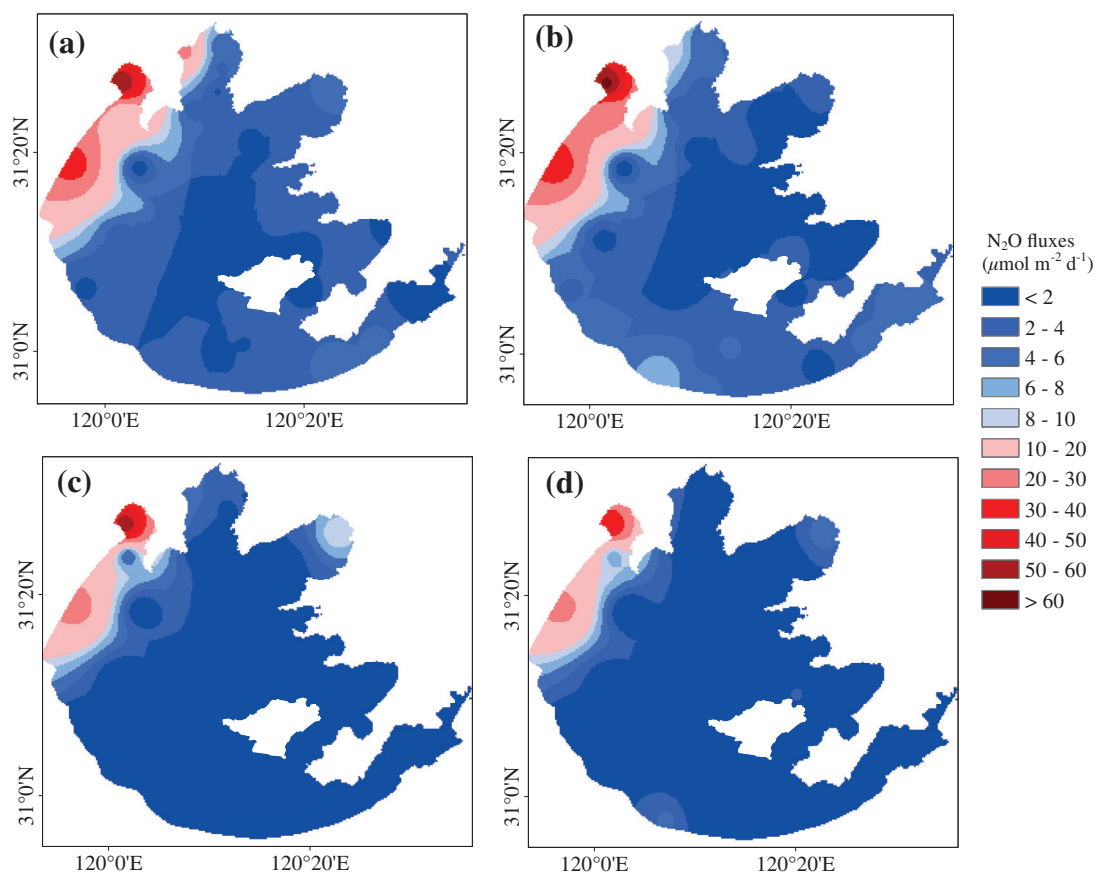


Fig. 5. Spatial variation in the N₂O fluxes in (a) spring (May), (b) summer (August), (c) autumn (November), and (d) winter (February). Data shown as the mean value during 2012–2016. [Color figure can be viewed at wileyonlinelibrary.com]

$p < 0.01$, $n = 460$), NH₄⁺-N ($r = 0.45$, $p < 0.01$, $n = 460$, $n = 448$), TN ($r = 0.46$, $p < 0.01$, $n = 448$), TP ($r = 0.43$, $p < 0.01$, $n = 448$), and DOC ($r = 0.23$, $p < 0.01$, $n = 448$) but

negatively correlated with DO ($r = -0.34$, $p < 0.01$, $n = 448$) and pH ($r = -0.14$, $p < 0.01$, $n = 448$). No significant correlations were found between the N₂O fluxes and Chl *a* nor

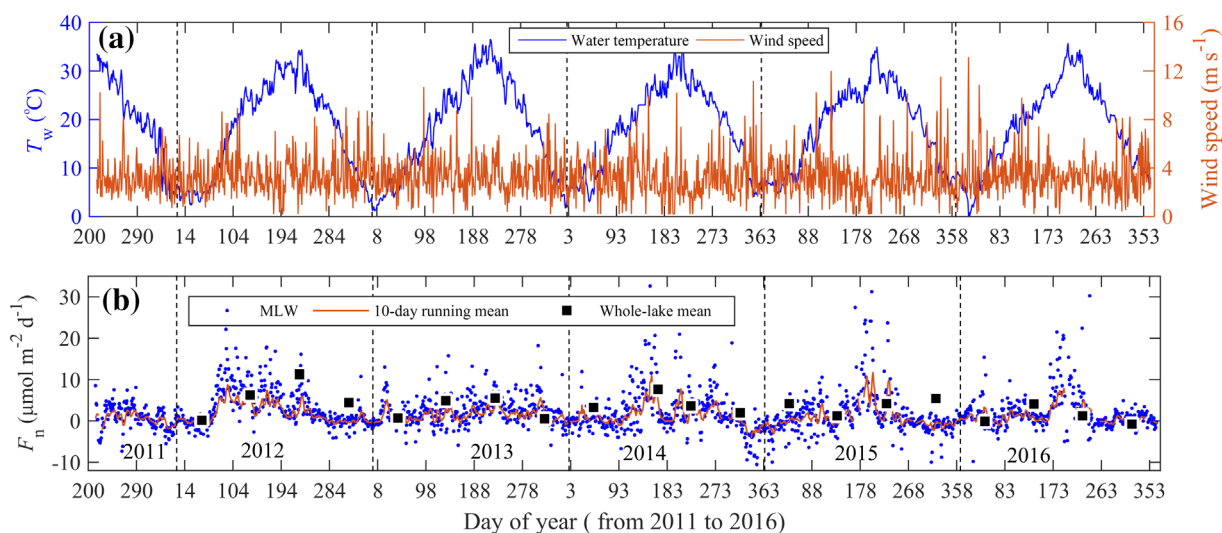


Fig. 6. Temporal variation in the meteorological factors and N₂O fluxes at the MLW site where daily water sampling took place. (a) Time series of water temperature (T_w , °C) and wind speed ($m s^{-1}$); (b) Temporal variation in the N₂O fluxes (F_n , $\mu mol m^{-2} d^{-1}$). Black squares indicate the whole-lake mean N₂O fluxes. Measurement locations are shown in Fig. 1. [Color figure can be viewed at wileyonlinelibrary.com]

Table 2. The annual mean N₂O fluxes (mean ± SD) for the three zones in Lake Taihu during 2012–2016.

Zone	Area (km ²)	F _n (μmol m ⁻² d ⁻¹)					Mean
		2012	2013	2014	2015	2016	
Zone 1	494	18.1 ± 10.2	9.0 ± 5.7	14.9 ± 8.1	11.1 ± 5.7	3.6 ± 2.5	11.4 ± 5.6
Zone 2	1397	2.4 ± 3.7	1.0 ± 2.3	1.1 ± 2.0	2.2 ± 1.4	0.4 ± 2.4	1.4 ± 0.9
Zone 3	447	1.3 ± 2.5	2.3 ± 2.1	1.7 ± 2.4	0.6 ± 0.6	0.6 ± 1.7	1.3 ± 0.7
Whole lake	2338	5.5 ± 4.8	2.9 ± 3.0	4.1 ± 3.4	3.8 ± 2.1	1.1 ± 2.3	3.5 ± 1.8

between the N₂O fluxes and ORP (Table 4). In addition, the seasonal N₂O fluxes were correlated with NO₂⁻-N in zone 1 ($r = 0.62$, $p < 0.01$, $n = 16$) and zone 2 ($r = 0.56$, $p = 0.012$, $n = 16$). In zone 3, the seasonal variation in the N₂O fluxes was moderately correlated with DOC ($r = 0.48$, $p = 0.067$, $n = 15$; Supporting Information Fig. S6a). It should be noted that the seasonal N₂O fluxes in the three zones were positively correlated with the inputs of river water from the Taihu Basin (zone 1: $r = 0.54$, $p < 0.05$; zone 2: $r = 0.67$, $p < 0.01$; zone 3: $r = 0.51$, $p < 0.05$; Supporting Information Fig. S6b).

N₂O emission factor

The multiple-year averages of EF_a and EF_b were 0.19% and 0.18%, respectively. The spatial distribution of EF_b showed an opposite pattern to that of N loadings (Figs. 2, 8a), where EF_b decreased as the N loadings increased. The spatial variation in EF_b was positively correlated with the mass ratio of DOC : DIN (Fig. 8b). Zone 3, with abundant submerged biomass, had the highest EF_b and largest mass ratio of DOC : DIN (Table 1). In addition, the seasonal variations in EF_b were also correlated with the ratio of DOC : DIN in the three zones (zone 1: $r = 0.84$, $p < 0.01$, $n = 16$; zone 2: $r = 0.88$, $p < 0.01$, $n = 16$; zone 3: $r = 0.73$, $p < 0.01$, $n = 16$; Supporting Information Table S2). The EF_b showed seasonality: autumn (mean ± SD: 0.33% ± 0.05%) > summer (0.21% ± 0.01%) > winter (0.10% ± 0.04%) > spring (0.07% ± 0.04%). There were statistically significant differences ($p < 0.01$) in EF_b among autumn, summer, and winter, while there was no significant difference ($p = 0.49$) in EF_b between winter and spring.

Table 3. Linear regression equation between N₂O fluxes (y , μmol m⁻² d⁻¹) and water temperature (x , °C) in the three zones^{*}.

Zone	Regression equation
Zone 1	$y = 2.16(\pm 1.14)x - 27.73(\pm 7.24)$; $R^2 = 0.17$; $p = 0.073$
Zone 2	$y = 0.52(\pm 0.22)x - 8.06(\pm 1.11)$; $R^2 = 0.24$; $p = 0.028$
Zone 3	$y = 0.35(\pm 0.11)x - 4.96(\pm 0.70)$; $R^2 = 0.36$; $p = 0.005$
Whole lake	$y = 0.62(\pm 0.23)x - 7.63(\pm 1.69)$; $R^2 = 0.29$; $p = 0.015$

^{*}The total number of observations is 20, representing seasonal samplings between 2012 and 2016, for all the regression relations shown. The parameter bounds on the linear regression coefficients are one standard deviation.

Discussion

Consistencies with previous studies

Previous studies reported N₂O fluxes ranging from $-8 \mu\text{mol m}^{-2} \text{d}^{-1}$ to $64.7 \mu\text{mol m}^{-2} \text{d}^{-1}$, with a mean value of $2.9\text{--}3.4 \mu\text{mol m}^{-2} \text{d}^{-1}$ (Supporting Information Table S3). The N₂O fluxes reported in this study ranged from $-7.1 \mu\text{mol m}^{-2} \text{d}^{-1}$ to $152.7 \mu\text{mol m}^{-2} \text{d}^{-1}$, with a mean value of $3.5 \mu\text{mol m}^{-2} \text{d}^{-1}$, across the whole lake. The mean N₂O emission rate from Lake Taihu was similar to that from temperate lakes ($3.4 \mu\text{mol m}^{-2} \text{d}^{-1}$) and higher than that from high latitude lakes ($1.1 \mu\text{mol m}^{-2} \text{d}^{-1}$) reported by Soued et al. (2016). For comparison, the mean N₂O flux in Lake Kivu, a large and deep-tropical lake, was $0.43 \mu\text{mol m}^{-2} \text{d}^{-1}$ (Roland et al. 2017). However, the mean N₂O flux reported in this study agrees with the global median value ($3.9 \mu\text{mol m}^{-2} \text{d}^{-1}$) estimated by Hu et al. (2016).

The diurnal pattern observed is consistent with field measurements by Yan et al. (2012), Xia et al. (2013a), and Yang et al. (2015) and demonstrates that a single daytime sample can be representative of the daily average N₂O flux. This finding has been widely adopted for N₂O fluxes measurements in terrestrial ecosystems (Song et al. 2009). The limited diurnal variations reported in this study may be associated with the small lake temperature variations that occur over a single day. Diurnal patterns in lake N₂O fluxes are expected when the diurnal range in temperature is $> 10^\circ\text{C}$ (Yang et al. 2015), while the lake water temperature differences in Lake Taihu were less than 4.2°C based on the hourly measurements at the MLW site (Supporting Information Fig. S4).

A previous study by Wang et al. (2009) reported a much larger mean flux of $11.9 \mu\text{mol m}^{-2} \text{d}^{-1}$ for Lake Taihu, which is 240% higher than the flux in the present study. This large discrepancy may have been caused by two reasons. First, Wang et al. (2009) reported N₂O emissions for only summer, when the N₂O emissions are normally high (Wang et al. 2007; Hinshaw and Dahlgren 2013; Fig. 6b). Second, the study by Wang et al. (2009) reported fluxes when the N loading in Lake Taihu was much higher than the present. Long-term monitoring indicated that whole-lake NH₄⁺-N concentrations decreased from 0.39 mg L^{-1} in 2007 to 0.11 mg L^{-1} in 2016 (Supporting Information Fig. S7). The decreasing N loading in this study was consistent with previous studies that showed a

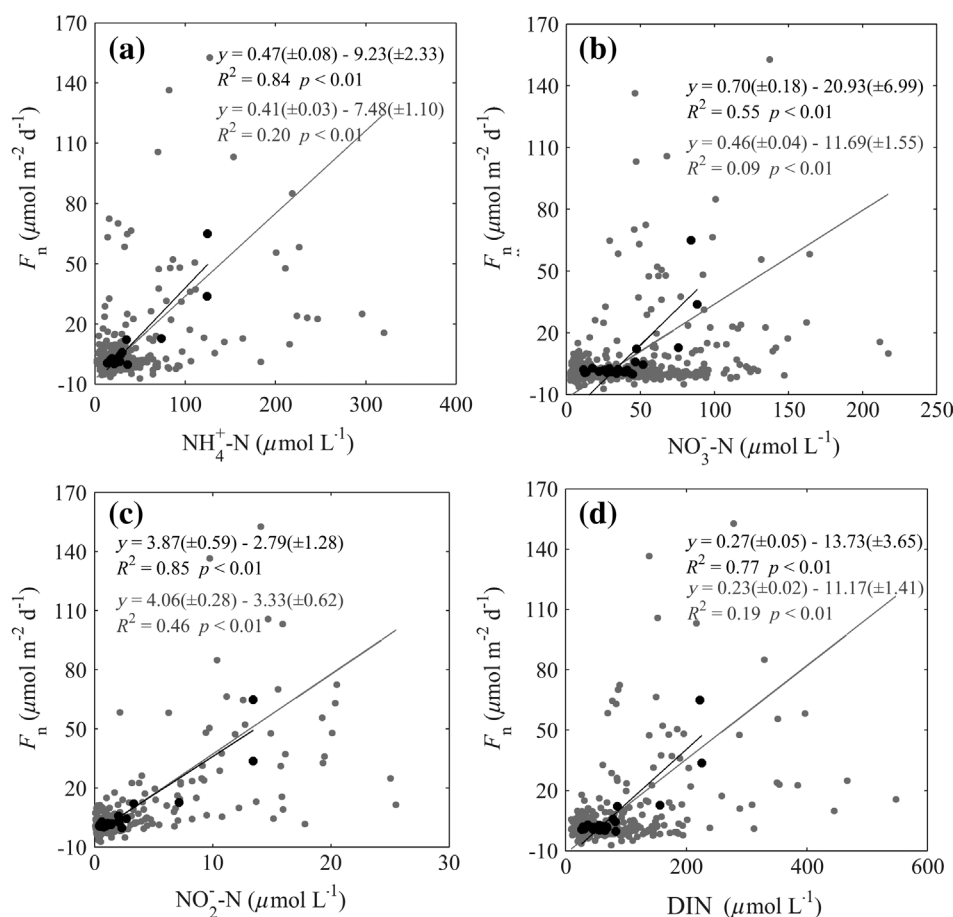


Fig. 7. Correlation of the N₂O fluxes and (a) NH₄⁺-N, (b) NO₃⁻-N, (c) NO₂⁻-N, and (d) DIN across Lake Taihu. Black points represent the mean values for each spatial sampling site during 2012–2015, and gray points represent all whole-lake survey data across space and time during 2012–2015. Parameter bounds on the regression coefficients are 95% confidence limits.

decline in Chinese lake N loading due to large government investments in environmental remediation (Tong et al. 2017; Zhou et al. 2017). Frequent eutrophication events have made Lake Taihu a priority environmental topic in China, leading to major environmental protection actions (e.g., the establishment of wastewater treatment plants) to reduce river pollutant discharge and improve the lake water quality (Duan

et al. 2009; Zhou et al. 2017). These actions may have directly contributed to the decrease in anthropogenic N loading input. The decreased N loading, along with the correlation shown in Fig. 7, may contribute to the moderate N₂O emissions of Lake Taihu reported here. The high-temporal variability documented in the present study emphasizes the importance of year-long monitoring sampling to achieve unbiased results. The

Table 4. Spatial Pearson correlation of the annual mean N₂O fluxes and water quality indices in different zones of the lake*.

	DO	pH	NO ₂ ⁻ -N	NO ₃ ⁻ -N	NH ₄ ⁺ -N	TP	TN	Spc	DOC	Chl <i>a</i>	ORP
All	-0.88 [†]	-0.67 [†]	0.92 [†]	0.75 [†]	0.92 [†]	0.72 [†]	0.79 [†]	0.59 [†]	0.56 [†]	0.27	0.18
Zone 1	-0.90 [†]	-0.75 [‡]	0.91 [†]	0.82 [†]	0.91 [†]	0.83 [†]	0.88 [†]	0.88 [‡]	0.71 [‡]	-0.21	0.31
Zone 2	-0.34	-0.76 [†]	0.59 [‡]	0.48	0.31	-0.27	-0.02	-0.54 [‡]	-0.79 [†]	-0.42	0.49
Zone 3	-0.34	-0.93 [†]	0.83 [†]	-0.01	0.26	0.29	0.17	-0.54	0.44	0.68	-0.06

*Chl *a*, chlorophyll *a* concentration; DO, dissolved oxygen concentration; DOC, dissolved organic carbon concentration; ORP, oxidation reduction potential; Spc, specific conductance; TN, total nitrogen concentration; TP, total phosphorus concentration. All, data acquired at all the spatial sampling sites ($n = 29$); Zone 1, data acquired at the eutrophic zone ($n = 9$); Zone 2, data acquired at the transitional zone ($n = 12$); Zone 3, data acquired at the submerged vegetation zone ($n = 8$).

[†]Correlation is significant at the 0.01 level.

[‡]Correlation is significant at the 0.05 level.

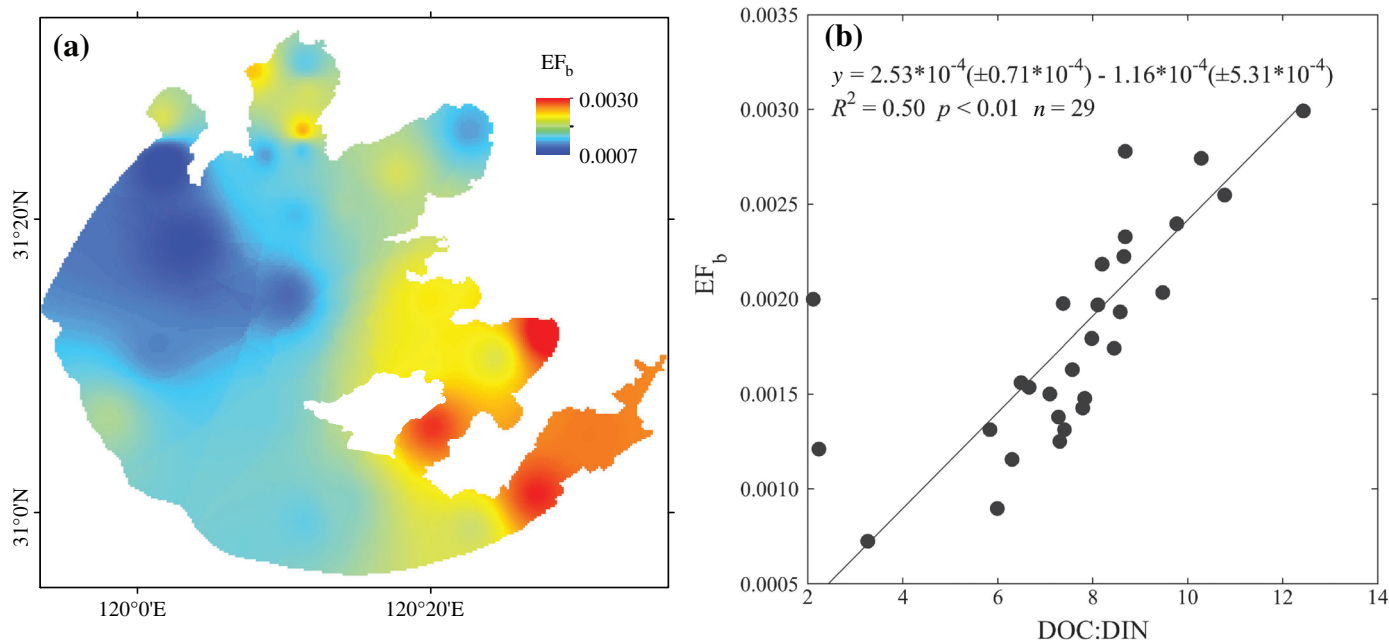


Fig. 8. (a) Map showing the spatial distribution of annual mean EF_b across Lake Taihu during 2012–2015 and (b) correlation between EF_b and the ratio of DOC concentration (mg L^{-1}) to DIN concentration (mg L^{-1}) (DOC : DIN) across Lake Taihu. Parameter bounds on the regression coefficients are 95% confidence limits. [Color figure can be viewed at wileyonlinelibrary.com]

continuity of environmental political management can also justify long-term high-frequency monitoring in lake environments (Tong et al. 2017; Zhou et al. 2017).

Given the large variability in observed fluxes across time and space, ranging from $-7.1 \mu\text{mol m}^{-2} \text{d}^{-1}$ to $152.7 \mu\text{mol m}^{-2} \text{d}^{-1}$, we extrapolated the Lake Taihu measurements to the whole basin lake ($\sim 3160 \text{ km}^2$) to estimate the annual budget of N₂O fluxes at the zonal base. We estimated that the whole basin lake emits approximately 113 Mg N of N₂O to the atmosphere yearly compared to the estimated basin-level riverine N₂O emissions of 1400 Mg yr⁻¹ (Wang et al. 2009; Yu et al. 2013; Xia et al. 2013a,b). For comparison, the estimated N₂O emissions from cultivated lands in the drainage basin are 12,000 Mg yr⁻¹ (Wang et al. 2009).

Coregulation of lake N₂O fluxes by N and temperature

The large differences in the N₂O fluxes between eutrophic zone 1 and zone 2 are an indication of the importance of nitrogen pollution in N₂O emissions. The mean N₂O flux in zone 1 was $11.4 \mu\text{mol m}^{-2} \text{d}^{-1}$, compared with $1.4 \mu\text{mol m}^{-2} \text{d}^{-1}$ in zone 2. Zone 1 received a majority of the river N discharge, while there were no direct river N inputs to zone 2 and zone 3 (Supporting Information Fig. S1; Xiao et al. 2017). Anthropogenic N inputs contributed to the substantial differences in N concentrations among the different zones. For example, the zonal mean of the NH₄⁺-N concentrations in zone 1 was 192% higher than that in zone 2 and zone 3.

Strong N control on N₂O fluxes can be further demonstrated by the positive correlation between N₂O fluxes and

NH₄⁺-N, NO₃⁻-N, and NO₂⁻-N concentrations (Table 4; Fig. 7). High N loading (NH₄⁺-N, NO₃⁻-N, and NO₂⁻-N) drives microbial processes of N₂O production. Lake Taihu receives anthropogenic N via river discharge and, therefore, contains high concentrations of N (Qin et al. 2007; Duan et al. 2009) that lead to enhanced N₂O emissions. This finding is consistent with previous studies, which reported that N₂O fluxes across the water–air interface were determined by N loading in aquatic ecosystems with external N inputs (Baulch et al. 2011; Beaulieu et al. 2011; Yu et al. 2013; Hama-Aziz et al. 2017; Borges et al. 2018). Given these strong positive correlations between N₂O and N in the water and the uniformly distributed water temperature, wind speed (wind-dependent gas transfer coefficient), and solar radiation (Wang et al. 2014; Xiao et al. 2017), the spatial variability in N₂O fluxes is primarily attributed to N loading in the lake.

The control of temperature on N₂O emissions in Lake Taihu is consistent with the control of temperature on microbial processes related to N₂O production (Beaulieu et al. 2010; Hinshaw and Dahlgren 2013). The lower water temperature may have contributed to the undersaturation of N₂O in winter (Fig. 6b). However, the importance of temperature control varied among the three zones (Table 3). In particular, the positive correlation between water temperature and N₂O emissions was significant in zone 2 and zone 3 and not significant in zone 1. The weak correlation between N₂O emissions and temperature in zone 1 shows the importance of N regulation for N₂O fluxes in eutrophic waters (Wang et al. 2007; Davidson et al. 2015).

The lake N₂O fluxes and N loading exhibited opposite seasonal patterns (Figs. 3, 5). High N concentrations in inflowing rivers occurred in summer due to the heavy application of fertilizers (Ju et al. 2009; Zhao et al. 2015), corresponding to relatively low N concentrations in the lake (Fig. 3d,e). This contrasting pattern is caused by the stimulation of N biogeochemical cycling by warm water temperatures (Beaulieu et al. 2010), which contributed to the larger N removal rates in the summer. In contrast, low-water temperatures in winter reduced these microbial processes, leading to N accumulation and low N₂O emissions. Our results, together with a previous study on the weak response of N₂O fluxes to N enrichment in boreal lakes (mean temperature: 1–3°C; Klaus et al. 2017), indicate that water temperature and N loading interactively control N₂O fluxes in Lake Taihu.

Controls of the lake N₂O EFs

EF_b showed a strong variation across the lake. The strong positive spatial correlation between the EF_b and DOC : DIN mass ratio (Fig. 8b) implied that higher DOC may enhance N₂O production, as suggested in previous studies (Xia et al. 2013a; Hu et al. 2016). The submerged macrophytes in zone 3 are a labile carbon source for N₂O production, which contributes to the high EF_b of this zone (Fig. 8a). Consistent with a few previous studies on rivers and streams (Mulholland et al. 2008; Beaulieu et al. 2011; Hinshaw and Dahlgren 2013; Hu et al. 2016), the EF_b reported here was also inversely correlated with N loadings (Figs. 2, 8a). This finding was attributed to decreasing microbial activity with increasing N inputs due to progressive biological saturation (Mulholland et al. 2008; Hu et al. 2016; Hampel et al. 2018). Both of these findings indicated that the variability in the N₂O EF was related to a range of factors, such as anthropogenic N inputs and DOC concentrations (Hu et al. 2016; Hama-Aziz et al. 2017).

There are some EF_b hot spots in zone 1, where algae biomass is abundant (Fig. 7a). Algal blooms likely enhanced the N₂O production by enhancing organic inputs (Chen et al. 2012). Field measurements showed that seasonal variations in the EF_b in zone 1 were correlated with Chl *a* ($r = 0.50$, $p = 0.05$, $n = 16$), an indicator of algal abundance. Algae may directly influence N₂O production in freshwater lakes by enhancing carbon inputs. A study showed that the previous year's winter temperature influences the algal blooming in Lake Taihu (Duan et al. 2009). An increase in the winter temperature over time was observed based on long-term continuous measurements in Lake Taihu during the sampling period (Fig. 3a; Lee et al. 2014); for example, the winter temperature in 2014, with a mean value of 6.2°C, was significantly ($p = 0.04$) higher than that in 2011 (mean value of 4.5°C). These findings not only explained the yearly increase in the Chl *a* maximum peaks, especially in eutrophic zone 1 (Fig. 3c) but also suggested that a climate-change-related increase in water temperature can influence lake N₂O production via stimulating algal blooming.

Environmental control of N₂O fluxes

The present study showed that the absence of submerged macrophytes had no significant effect on lake N₂O fluxes (Figs. 4, 5). The mean N₂O flux and dissolved N₂O concentration in zone 3, with abundant submerged macrophytes, were 1.3 $\mu\text{mol m}^{-2} \text{d}^{-1}$ and 11.8 nmol L^{-1} , respectively. For comparison, the values in zone 2 were 1.4 $\mu\text{mol m}^{-2} \text{d}^{-1}$ and 12.0 nmol L^{-1} , respectively. Our results are consistent with the field measurements by Yao et al. (2017), which reported that submerged macrophytes are not a primary factor in the spatial distribution of N₂O. A previous study showed that macrophytes could indirectly influence N₂O fluxes by altering the DIN concentrations and oxygen availability in aquatic ecosystems (Murray et al. 2015). However, the concentrations of DIN and DO in Lake Taihu showed small differences between zone 2, with an absence of submerged macrophytes, and zone 3, with abundant submerged macrophytes (Fig. 2). Additionally, our field measurements showed that beyond the threshold of the DOC : DIN mass ratio (3–5), surface N₂O concentrations and N₂O fluxes variabilities in the lake had stable trends with an increasing DOC : DIN mass ratio (Supporting Information Fig. S8). The mean DOC : DIN mass ratios were 7.03 and 9.64 (Table 1) in zone 2 and zone 3, respectively. Both of these may have contributed to the observed results in the lake.

N₂O fluxes are driven by the microbial processes of nitrification and denitrification in aquatic ecosystems. The water column remains well oxygenated in the shallow Lake Taihu (Supporting Information Fig. S9; Hu et al. 2015), indicating denitrification cannot occur in the water column (Zhang et al. 2010), while the high concentrations of DO and NH₄⁺-N provide favorable conditions for the occurrence of nitrification (Zhang et al. 2010; Whitfield et al. 2011; Hampel et al. 2018). The observed fluxes were highly correlated with NH₄⁺-N and NO₂⁻-N (Fig. 7), which also confirmed that nitrification dominated N₂O production in the lake (Yu et al. 2013). A previous study showed that the nitrification rates of the water column at the eutrophic sampling site in Lake Taihu were significantly higher fueled by high NH₄⁺-N concentrations (Hampel et al. 2018), and this finding may have contributed to the higher N₂O fluxes in eutrophic zone 1 (Figs. 4, 5). Some N₂O peaks occurred in the bottom water in May 2013 based on the N₂O vertical profile measurements at MLW (Supporting Information Fig. S2c,d), which suggest that denitrification could occur in the sediments and thus contribute to lake N₂O production (Xu et al. 2010; Zhang et al. 2010).

Previous studies have reported that low pH may limit nitrification rates and reduce aquatic N₂O emissions (Beman et al. 2011; Soued et al. 2016). But negative relationship between the pH and N₂O fluxes was found in Lake Taihu (Table 4). Also, a significant positive correlation between the N₂O fluxes and DO was expected in the lake water if N₂O was primarily produced via the nitrification process (Yu et al. 2013). However, our results showed that the N₂O fluxes were negatively correlated with DO concentrations ($r = -0.34$, $p < 0.01$,

$n = 448$) in the lake, consistent with previous measurements in rivers with external N loading (Rosamond et al. 2012; Yu et al. 2013). These results indicated N₂O production in the lake was favored under low DO and low pH due to the high anthropogenic N inputs, which was consistent with field measurements in rivers in eastern China (Yu et al. 2013).

Conclusions, implications, and perspectives

With a 5-yr continuous measurement period of N₂O concentrations and fluxes, we quantified the budget of N₂O fluxes and investigated their spatial and temporal variations in Lake Taihu. The annual mean N₂O flux of this eutrophic lake was $3.5 \pm 1.8 \mu\text{mol m}^{-2} \text{d}^{-1}$, with an annual N₂O budget of $134.4 \pm 69.8 \text{ Mg } (10^6 \text{ g}) \text{ yr}^{-1}$, suggesting that Lake Taihu is a moderate source of atmospheric N₂O compared to other inland lakes worldwide.

The highest N₂O fluxes occurred in the eutrophic zone, where anthropogenic N inputs were high. The lowest N₂O fluxes occurred in noneutrophic zones that received no river nutrient inputs. N inputs and temperature coregulated the variations in N₂O fluxes from Lake Taihu. The observed fluxes were highly correlated with NH₄⁺-N and NO₂⁻-N concentrations, with respect to lower correlations to NO₃⁻-N concentrations. This indicates that nitrification is an important process regulating N₂O in the lake. The temporal variations in the observed fluxes were primarily regulated by water temperature.

Previous studies proposed that N₂O emissions from aquatic ecosystems in eastern China were high due to high anthropogenic N loading (Seitzinger and Kroeze 1998; Seitzinger et al. 2000). For example, agricultural N fertilizer use alone within the study areas has reached $550 \text{ kg N ha}^{-1} \text{ yr}^{-1}$, and 50–80% of this anthropogenic N is lost to waters (Xing and Zhu 2002; Ju et al. 2009). For comparison, N fertilizer use in the US Corn Belt, an intensive agricultural region, was $100 \text{ kg N ha}^{-1} \text{ yr}^{-1}$ (Turner et al. 2015; Griffis et al. 2017). Given the significant positive correlations between N₂O fluxes and N loading (Table 4; Fig. 7), the reported moderate N₂O emissions from Lake Taihu from 2012 to 2016 were probably due to the decrease in N loading, especially in zone 1 (Supporting Information Figs. S7, S10). The high temporal and spatial variabilities reported here highlight the importance of long-term and spatially distributed sampling to achieve unbiased results.

Long-term field measurements of N₂O fluxes in the highly heterogeneous Lake Taihu will shed further light on the effect of basin and lake management on N₂O emissions from freshwater lakes. Additionally, eutrophication and global warming would enhance lake N₂O emissions given the coregulation of N₂O fluxes by anthropogenic N input and water temperature. This study, to the best of our knowledge, represents the first attempt to quantify lake N₂O fluxes at such a high temporal and spatial resolution. The results show that Lake Taihu is a moderate source of atmospheric N₂O and provide new

insights into the biogeochemistry of Lake Taihu, the third largest freshwater lake in China. The results provide a valuable data source for model development and validation to project N₂O fluxes from fresh waterbodies under a changing environment.

The N₂O EFs reported in the lake were comparable to the global mean EFs of 0.17% from riverine ecosystems (Hu et al. 2016). The minor difference between EF_a and EF_b in this study was probably due to the thorough temporal and spatial sampling strategy (Outram and Hiscock 2012; Hama-Aziz et al. 2017). Previous studies reported EF_b ranging from 0.03% to 1% (McCrackin and Elser 2011; Outram and Hiscock 2012). In addition, different EFs for different water types within the same catchment have been reported (Outram and Hiscock 2012). Our data showed that EFs varied spatially within one lake along gradients of N enrichment and submerged macrophytes (Fig. 8a).

The annual mean net anthropogenic N input to Lake Taihu was approximately $0.03 \text{ Tg N yr}^{-1}$ (Supporting Information Table S1), but the proportion of transported N converted to N₂O was unknown. Our results reported here show that only 0.30% of the net N input was lost as N₂O. Taking the national total N₂O emissions as 2150 Gg yr^{-1} (Zhou et al. 2014), the N₂O emissions from Lake Taihu accounted for 0.006% of the national N₂O budget across China. Considering the large N flow into Lake Taihu (Supporting Information Table S1, Fig. 2), the relatively low N₂O emissions may be attributed to the shallow depth of the lake, which may limit the space for the development of microbial communities, and to the well-oxygenated water, which prevent the occurrence of denitrification. Nitrification and denitrification rates should be measured in future studies of Lake Taihu to have a more complete quantification of N cycles.

References

- American Public Health Association. 1995. Standard methods for the examination of water and wastewater, 19th ed. APHA, American Water Works Association, Water Environment Federation.
- Baulch, H., S. Schiff, R. Maranger, and P. Dillon. 2011. Nitrogen enrichment and the emission of nitrous oxide from streams. *Global Biogeochem. Cycles* **25**: GB4013. doi:10.1029/2011GB004047
- Beaulieu, J. J., W. D. Shuster, and J. A. Rebolz. 2010. Nitrous oxide emissions from a large, impounded river: The Ohio River. *Environ. Sci. Technol.* **44**: 7527–7533. doi:10.1021/es1016735
- Beaulieu, J. J., and others. 2011. Nitrous oxide emission from denitrification in stream and river networks. *Proc. Natl. Acad. Sci. USA* **108**: 214–219. doi:10.1073/pnas.1011464108
- Beman, J. M., and others. 2011. Global declines in oceanic nitrification rates as a consequence of ocean acidification.

- Proc. Natl. Acad. Sci. USA **108**: 208–213. doi:[10.1073/pnas.1011053108](https://doi.org/10.1073/pnas.1011053108)
- Borges, A. V., and others. 2015. Globally significant greenhouse-gas emissions from African inland waters. *Nat. Geosci.* **8**: 637–642. doi:[10.1038/ngeo2486](https://doi.org/10.1038/ngeo2486)
- Borges, A. V., and others. 2018. Effects of agricultural land use on fluvial carbon dioxide, methane and nitrous oxide concentrations in a large European river, the Meuse (Belgium). *Sci. Total Environ.* **610**: 342–355. doi:[10.1016/j.scitotenv.2017.08.047](https://doi.org/10.1016/j.scitotenv.2017.08.047)
- Chapuis-Lardy, L., N. Wrage, A. Metay, J.-L. Chotte, and M. Bernoux. 2007. Soils, a sink for N₂O? A review. *Glob. Chang. Biol.* **13**: 1–17. doi:[10.1111/j.1365-2486.2006.01280.x](https://doi.org/10.1111/j.1365-2486.2006.01280.x)
- Chen, X. F., L. Y. Yang, L. Xiao, A. J. Miao, and B. D. Xi. 2012. Nitrogen removal by denitrification during cyanobacterial bloom in Lake Taihu. *J. Freshw. Ecol.* **27**: 243–258. doi:[10.1080/02705060.2011.644405](https://doi.org/10.1080/02705060.2011.644405)
- Cole, J. J., and N. F. Caraco. 1998. Atmospheric exchange of carbon dioxide in a low-wind oligotrophic lake measured by the addition of SF₆. *Limnol. Oceanogr.* **43**: 647–656. doi:[10.4319/lo.1998.43.4.0647](https://doi.org/10.4319/lo.1998.43.4.0647)
- Davidson, E. A. 2009. The contribution of manure and fertilizer nitrogen to atmospheric nitrous oxide since 1860. *Nat. Geosci.* **2**: 659–662. doi:[10.1038/ngeo608](https://doi.org/10.1038/ngeo608)
- Davidson, T. A., and others. 2015. Eutrophication effects on greenhouse gas fluxes from shallow-lake mesocosms override those of climate warming. *Glob. Chang. Biol.* **21**: 4449–4463. doi:[10.1111/gcb.13062](https://doi.org/10.1111/gcb.13062)
- De Klein, C., and others. 2006. Chapter 11: N₂O emissions from managed soils, and CO₂ emissions from lime and urea application, p. 1–54. *In* IPCC guidelines for national greenhouse gas inventories. Prepared by the National Greenhouse Gas Inventories Programme, v. **4**. Institute for Global Environmental Strategies.
- Duan, H., R. Ma, S. A. Loiselle, Q. Shen, H. Yin, and Y. Zhang. 2014. Optical characterization of black water blooms in eutrophic waters. *Sci. Total Environ.* **482**: 174–183. doi:[10.1016/j.scitotenv.2014.02.113](https://doi.org/10.1016/j.scitotenv.2014.02.113)
- Duan, H. T., and others. 2009. Two-decade reconstruction of algal blooms in China's Lake Taihu. *Environ. Sci. Technol.* **43**: 3522–3528. doi:[10.1021/es8031852](https://doi.org/10.1021/es8031852)
- Ebina, J., T. Tsutsui, and T. Shirai. 1983. Simultaneous determination of total nitrogen and total phosphorus in water using peroxodisulfate oxidation. *Water Res.* **17**: 1721–1726. doi:[10.1016/0043-1354\(83\)90192-6](https://doi.org/10.1016/0043-1354(83)90192-6)
- Foley, J., D. de Haas, Z. Yuan, and P. Lant. 2010. Nitrous oxide generation in full-scale biological nutrient removal wastewater treatment plants. *Water Res.* **44**: 831–844. doi:[10.1016/j.watres.2009.10.033](https://doi.org/10.1016/j.watres.2009.10.033)
- Fu, C., X. Lee, T. Griffis, J. Baker, and P. Turner. 2018. A modeling study of direct and indirect N₂O emissions from a representative catchment in the U.S. Corn Belt. *Water Resour. Res.* **54**: 3632–3653. doi:[10.1029/2017WR022108](https://doi.org/10.1029/2017WR022108)
- Griffis, T. J., and others. 2017. Nitrous oxide emissions are enhanced in a warmer and wetter world. *Proc. Natl. Acad. Sci. USA* **114**: 12081–12085. doi:[10.1073/pnas.1704552114](https://doi.org/10.1073/pnas.1704552114)
- Hama-Aziz, Z. Q., K. M. Hiscock, and R. J. Cooper. 2017. Indirect nitrous oxide emission factors for agricultural field drains and headwater streams. *Environ. Sci. Technol.* **51**: 301–307. doi:[10.1021/acs.est.6b05094](https://doi.org/10.1021/acs.est.6b05094)
- Hampel, J. J., M. McCarthy, W. Gardner, L. Zhang, H. Xu, G. Zhu, and S. Newell. 2018. Nitrification and ammonium dynamics in Taihu Lake, China: Seasonal competition for ammonium between nitrifiers and cyanobacteria. *Biogeosciences* **15**: 733–748. doi:[10.5194/bg-15-733-2018](https://doi.org/10.5194/bg-15-733-2018)
- Harrison, J. A., and others. 2009. The regional and global significance of nitrogen removal in lakes and reservoirs. *Biogeochemistry* **93**: 143–157. doi:[10.1007/s10533-008-9272-x](https://doi.org/10.1007/s10533-008-9272-x)
- Hinshaw, S. E., and R. A. Dahlgren. 2013. Dissolved nitrous oxide concentrations and fluxes from the eutrophic San Joaquin River, California. *Environ. Sci. Technol.* **47**: 1313–1322. doi:[10.1021/es301373h](https://doi.org/10.1021/es301373h)
- Hu, M., D. Chen, and R. A. Dahlgren. 2016. Modeling nitrous oxide (N₂O) emission from rivers: A global assessment. *Glob. Chang. Biol.* **22**: 3566–3582. doi:[10.1111/gcb.13351](https://doi.org/10.1111/gcb.13351)
- Hu, Z., Q. Xiao, J. Yang, W. Xiao, W. Wang, S. Liu, and X. Lee. 2015. Temporal dynamics and drivers of ecosystem metabolism in a large subtropical shallow lake (Lake Taihu). *Int. J. Environ. Res. Public Health* **12**: 3691–3706. doi:[10.3390/ijerph120403691](https://doi.org/10.3390/ijerph120403691)
- Huttunen, J. T., and others. 2003. Fluxes of methane, carbon dioxide and nitrous oxide in boreal lakes and potential anthropogenic effects on the aquatic greenhouse gas emissions. *Chemosphere* **52**: 609–621. doi:[10.1016/s0045-6535\(03\)00243-1](https://doi.org/10.1016/s0045-6535(03)00243-1)
- IPCC. 2013. Climate change 2013: The physical science basis, p. 53–54. *In* T. F. Stocker, D. Qin, G. K. Plattner, M. Tignor, S. K. Allen, J. Boschung, A. Nauels, Y. Xia, V. Bex, and P. M. Midgley [eds.], Contribution of working group I to the fifth assessment report of the Intergovernmental Panel on Climate Change. Cambridge Univ. Press.
- Ivens, W. P. M. F., D. J. J. Tysmans, C. Kroeze, A. J. Löhr, and J. van Wijnen. 2011. Modeling global N₂O emissions from aquatic systems. *Curr. Opin. Environ. Sustain.* **3**: 350–358. doi:[10.1016/j.cosust.2011.07.007](https://doi.org/10.1016/j.cosust.2011.07.007)
- Ju, X. T., and others. 2009. Reducing environmental risk by improving N management in intensive Chinese agricultural systems. *Proc Natl Acad Sci USA* **106**: 3041–3046. doi:[10.1073/pnas.0813417106](https://doi.org/10.1073/pnas.0813417106)
- Kampschreur, M., H. Temmink, R. Kleerebezem, M. Jetten, and M. van Loosdrecht. 2009. Nitrous oxide emission during wastewater treatment. *Water Res.* **43**: 4093–4103. doi:[10.1016/j.watres.2009.03.001](https://doi.org/10.1016/j.watres.2009.03.001)
- Klaus, M., A.-K. Bergström, A. Jonsson, A. Deininger, E. Gebrink, and J. Karlsson. 2017. Weak response of greenhouse gas emissions to whole lake N enrichment. *Limnol. Oceanogr.* **63**: S340–S353. doi:[10.1002/lno.10743](https://doi.org/10.1002/lno.10743)

- Lee, X., and others. 2014. The Taihu eddy flux network: An observational program on energy, water and greenhouse gas fluxes of a large freshwater lake. *Bull. Am. Meteorol. Soc.* **95**: 1583–1594. doi:[10.1175/bams-d-13-00136.1](https://doi.org/10.1175/bams-d-13-00136.1)
- Liu, W., L. Yao, X. Jiang, L. Guo, X. Cheng, and G. Liu. 2017. Sediment denitrification in Yangtze lakes is mainly influenced by environmental conditions but not biological communities. *Sci. Total Environ.* **616-617**: 978–987. doi:[10.1016/j.scitotenv.2017.10.221](https://doi.org/10.1016/j.scitotenv.2017.10.221)
- Luo, J., and others. 2016. Applying remote sensing techniques to monitoring seasonal and interannual changes of aquatic vegetation in Taihu Lake, China. *Ecol. Indic.* **60**: 503–513. doi:[10.1016/j.ecolind.2015.07.029](https://doi.org/10.1016/j.ecolind.2015.07.029)
- MacIntyre, S., A. Jonsson, M. Jansson, J. Aberg, D. E. Turney, and S. D. Miller. 2010. Buoyancy flux, turbulence, and the gas transfer coefficient in a stratified lake. *Geophys. Res. Lett.* **37**. doi:[10.1029/2010gl044164](https://doi.org/10.1029/2010gl044164)
- McCrackin, M. L., and J. J. Elser. 2011. Greenhouse gas dynamics in lakes receiving atmospheric nitrogen deposition. *Global Biogeochem. Cycles* **25**. doi:[10.1029/2010gb003897](https://doi.org/10.1029/2010gb003897)
- Mengis, M., R. Gächter, and B. Wehrli. 1996. Nitrous oxide emissions to the atmosphere from an artificially oxygenated lake. *Limnol. Oceanogr.* **41**: 548–553. doi:[10.4319/lo.1996.41.3.0548](https://doi.org/10.4319/lo.1996.41.3.0548)
- Mengis, M., R. Gächter, and B. Wehrli. 1997. Sources and sinks of nitrous oxide (N₂O) in deep lakes. *Biogeochemistry* **38**: 281–301. doi:[10.1023/A:1005814020322](https://doi.org/10.1023/A:1005814020322)
- Miettinen, H., J. Pumpanen, J. Heiskanen, H. Aaltonen, I. Mammarella, A. Ojala, J. Levula, and M. Rantakari. 2015. Towards a more comprehensive understanding of lacustrine greenhouse gas dynamics—two-year measurements of concentrations and fluxes of CO₂, CH₄ and N₂O in a typical boreal lake surrounded by managed forests. *Boreal Environ. Res.* **20**: 75–89.
- Mulholland, P. J., and others. 2008. Stream denitrification across biomes and its response to anthropogenic nitrate loading. *Nature* **452**: 202–205. doi:[10.1038/nature06686](https://doi.org/10.1038/nature06686)
- Murray, R. H., D. V. Erler, and B. D. Eyre. 2015. Nitrous oxide fluxes in estuarine environments: Response to global change. *Glob. Chang. Biol.* **21**: 3219–3245. doi:[10.1111/gcb.12923](https://doi.org/10.1111/gcb.12923)
- Outram, F. N., and K. M. Hiscock. 2012. Indirect nitrous oxide emissions from surface water bodies in a lowland arable catchment: A significant contribution to agricultural greenhouse gas budgets? *Environ. Sci. Technol.* **46**: 8156–8163. doi:[10.1021/es3012244](https://doi.org/10.1021/es3012244)
- Qin, B., P. Xu, Q. Wu, L. Luo, and Y. Zhang. 2007. Environmental issues of Lake Taihu, China. *Hydrobiologia* **581**: 3–14. doi:[10.1007/s10750-006-0521-5](https://doi.org/10.1007/s10750-006-0521-5)
- Ravishankara, A. R., J. S. Daniel, and R. W. Portmann. 2009. Nitrous oxide (N₂O): The dominant ozone-depleting substance emitted in the 21st century. *Science* **326**: 123–125. doi:[10.1126/science.1176985](https://doi.org/10.1126/science.1176985)
- Read, J. S., and others. 2012. Lake-size dependency of wind shear and convection as controls on gas exchange. *Geophys. Res. Lett.* **39**: 39. doi:[10.1029/2012gl051886](https://doi.org/10.1029/2012gl051886)
- Roland, F. A., F. Darchambeau, C. Morana, and A. Borges. 2017. Nitrous oxide and methane seasonal variability in the epilimnion of a large tropical meromictic lake (Lake Kivu, East-Africa). *Aquat. Sci.* **79**: 209–218. doi:[10.1007/s00027-016-0491-2](https://doi.org/10.1007/s00027-016-0491-2)
- Rosamond, M. S., S. J. Thuss, and S. L. Schiff. 2012. Dependence of riverine nitrous oxide emissions on dissolved oxygen levels. *Nat. Geosci.* **5**: 715–718. doi:[10.1038/ngeo1556](https://doi.org/10.1038/ngeo1556)
- Saikawa, E., and others. 2014. Global and regional emissions estimates for N₂O. *Atmos. Chem. Phys.* **14**: 4617–4641. doi:[10.5194/acp-14-4617-2014](https://doi.org/10.5194/acp-14-4617-2014)
- Seitzinger, S., and others. 2006. Denitrification across landscapes and waterscapes: A synthesis. *Ecol. Appl.* **16**: 2064–2090. doi:[10.1890/1051-0761\(2006\)016\[2064:DALAWA\]2.0.CO;2](https://doi.org/10.1890/1051-0761(2006)016[2064:DALAWA]2.0.CO;2)
- Seitzinger, S. P., and C. Kroeze. 1998. Global distribution of nitrous oxide production and N inputs in freshwater and coastal marine ecosystems. *Global Biogeochem. Cycles* **12**: 93–113. doi:[10.1029/97gb03657](https://doi.org/10.1029/97gb03657)
- Seitzinger, S. P., C. Kroeze, and R. V. Styles. 2000. Global distribution of N₂O emissions from aquatic systems: Natural emissions and anthropogenic effects. *Chemosphere Glob. Chang. Sci.* **2**: 267–279.
- Sinha, E., A. M. Michalak, and V. Balaji. 2017. Eutrophication will increase during the 21st century as a result of precipitation changes. *Science* **357**: 405–408. doi:[10.1126/science.aan2409](https://doi.org/10.1126/science.aan2409)
- Song, C., X. Xu, H. Tian, and Y. Wang. 2009. Ecosystem-atmosphere exchange of CH₄ and N₂O and ecosystem respiration in wetlands in the Sanjiahe Plain, Northeastern China. *Glob. Chang. Biol.* **15**: 692–705. doi:[10.1111/j.1365-2486.2008.01821.x](https://doi.org/10.1111/j.1365-2486.2008.01821.x)
- Soued, C., P. A. del Giorgio, and R. Maranger. 2016. Nitrous oxide sinks and emissions in boreal aquatic networks in Québec. *Nat. Geosci.* **9**: 116–120. doi:[10.1038/ngeo2611](https://doi.org/10.1038/ngeo2611)
- Tong, Y., and others. 2017. Decline in Chinese lake phosphorus concentration accompanied by shift in sources since 2006. *Nat. Geosci.* **10**: 507–511. doi:[10.1038/NGEO2967](https://doi.org/10.1038/NGEO2967)
- Turner, P. A., T. J. Griffis, X. Lee, J. M. Baker, R. T. Venterea, and J. D. Wood. 2015. Indirect nitrous oxide emissions from streams within the US Corn Belt scale with stream order. *Proc. Natl. Acad. Sci. USA* **112**: 9839–9843. doi:[10.1073/pnas.1503598112](https://doi.org/10.1073/pnas.1503598112)
- Wang, H., L. Yang, W. Wang, J. Lu, and C. Yin. 2007. Nitrous oxide (N₂O) fluxes and their relationships with water-sediment characteristics in a hyper-eutrophic shallow lake, China. *J. Geophys. Res. Biogeosci.* **112**. doi:[10.1029/2005jg000129](https://doi.org/10.1029/2005jg000129)
- Wang, S. L., and others. 2009. The spatial distribution and emission of nitrous oxide (N₂O) in a large eutrophic lake in eastern China: Anthropogenic effects. *Sci. Total Environ.* **407**: 3330–3337. doi:[10.1016/j.scitotenv.2008.10.037](https://doi.org/10.1016/j.scitotenv.2008.10.037)

- Wang, W., and others. 2014. Temporal and spatial variations in radiation and energy balance across a large freshwater lake in China. *J. Hydrol.* **511**: 811–824. doi:[10.1016/j.jhydrol.2014.02.012](https://doi.org/10.1016/j.jhydrol.2014.02.012)
- Whitfield, C. J., J. Aherne, and H. M. Baulch. 2011. Controls on greenhouse gas concentrations in polymictic headwater lakes in Ireland. *Sci. Total Environ.* **410**: 217–225. doi:[10.1016/j.scitotenv.2011.09.045](https://doi.org/10.1016/j.scitotenv.2011.09.045)
- Xia, Y., Y. Li, X. Li, M. Guo, D. She, and X. Yan. 2013a. Diurnal pattern in nitrous oxide emissions from a sewage-enriched river. *Chemosphere* **92**: 421–428. doi:[10.1016/j.chemosphere.2013.01.038](https://doi.org/10.1016/j.chemosphere.2013.01.038)
- Xia, Y. Q., Y. F. Li, C. P. Ti, X. B. Li, Y. Q. Zhao, and X. Y. Yan. 2013b. Is indirect N₂O emission a significant contributor to the agricultural greenhouse gas budget? A case study of a rice paddy-dominated agricultural watershed in eastern China. *Atmos. Environ.* **77**: 943–950. doi:[10.1016/j.atmosenv.2013.06.022](https://doi.org/10.1016/j.atmosenv.2013.06.022)
- Xiao, Q., and others. 2017. Spatial variations of methane emission in a large shallow eutrophic lake in subtropical climate. *J. Geophys. Res. Biogeosci.* **122**: 1597–1614. doi:[10.1002/2017jg003805](https://doi.org/10.1002/2017jg003805)
- Xing, G. X., and Z. L. Zhu. 2002. Regional nitrogen budgets for China and its major watersheds. *Biogeochemistry* **57**: 405–427. doi:[10.1023/a:1016508323200](https://doi.org/10.1023/a:1016508323200)
- Xu, H., H. W. Paerl, B. Qin, G. Zhu, and G. Gao. 2010. Nitrogen and phosphorus inputs control phytoplankton growth in eutrophic Lake Taihu, China. *Limnol. Oceanogr.* **55**: 420–432. doi:[10.4319/lo.2010.55.1.0420](https://doi.org/10.4319/lo.2010.55.1.0420)
- Xu, X., H. Tian, and D. Hui. 2008. Convergence in the relationship of CO₂ and N₂O exchanges between soil and atmosphere within terrestrial ecosystems. *Glob. Chang. Biol.* **14**: 1651–1660. doi:[10.1111/j.1365-2486.2008.01595.x](https://doi.org/10.1111/j.1365-2486.2008.01595.x)
- Yan, W. J., L. B. Yang, F. Wang, J. N. Wang, and P. Ma. 2012. Riverine N₂O concentrations, exports to estuary and emissions to atmosphere from the Changjiang River in response to increasing nitrogen loads. *Global Biogeochem. Cycles* **26**: 15. doi:[10.1029/2010gb003984](https://doi.org/10.1029/2010gb003984)
- Yang, M., and others. 2015. N₂O fluxes from the littoral zone of a Chinese reservoir. *Biogeosciences* **12**: 4711–4723. doi:[10.5194/bg-12-4711-2015](https://doi.org/10.5194/bg-12-4711-2015)
- Yao, L., C. Chen, G. Liu, and W. Liu. 2017. Sediment nitrogen cycling rates and microbial abundance along a submerged vegetation gradient in a eutrophic lake. *Sci. Total Environ.* **616–617**: 899–907. doi:[10.1016/j.scitotenv.2017.10.230](https://doi.org/10.1016/j.scitotenv.2017.10.230)
- Yu, Z., and others. 2013. Nitrous oxide emissions in the Shanghai river network: Implications for the effects of urban sewage and IPCC methodology. *Glob. Chang. Biol.* **19**: 2999–3010. doi:[10.1111/gcb.12290](https://doi.org/10.1111/gcb.12290)
- Zhang, G., J. Zhang, S. Liu, J. Ren, and Y. Zhao. 2010. Nitrous oxide in the Changjiang (Yangtze River) Estuary and its adjacent marine area: Riverine input, sediment release and atmospheric fluxes. *Biogeosciences* **7**: 3505–3516. doi:[10.5194/bg-7-3505-2010](https://doi.org/10.5194/bg-7-3505-2010)
- Zhang, Y., and others. 2017. Global loss of aquatic vegetation in lakes. *Earth Sci. Rev.* **173**: 259–265. doi:[10.1016/j.earscirev.2017.08.013](https://doi.org/10.1016/j.earscirev.2017.08.013)
- Zhao, Y., Y. Xia, C. Ti, J. Shan, B. Li, L. Xia, and X. Yan. 2015. Nitrogen removal capacity of the river network in a high nitrogen loading region. *Environ. Sci. Technol.* **49**: 1427–1435. doi:[10.1021/es504316b](https://doi.org/10.1021/es504316b)
- Zhou, F., and others. 2014. A new high-resolution N₂O emission inventory for China in 2008. *Environ. Sci. Technol.* **48**: 8538–8547. doi:[10.1021/es5018027](https://doi.org/10.1021/es5018027)
- Zhou, Y., and others. 2017. Improving water quality in China: Environmental investment pays dividends. *Water Res.* **118**: 152–159. doi:[10.1016/j.watres.2017.04.035](https://doi.org/10.1016/j.watres.2017.04.035)
- Zhu, D., and others. 2015. Nitrous oxide emission from infralittoral zone and pelagic zone in a shallow lake: Implications for whole lake flux estimation and lake restoration. *Ecol. Eng.* **82**: 368–375. doi:[10.1016/j.ecoleng.2015.05.032](https://doi.org/10.1016/j.ecoleng.2015.05.032)

Acknowledgments

We are grateful for the constructive comments from the journal reviewers, the editors Maren Voss and Robert Howarth, and Steven Loisel (University of Siena, Italy). We would like to thank the Chinese Ecosystem Research Network (CERN), Taihu Laboratory for Lake Ecosystem Research, for providing water chemistry data. This research was funded jointly by the National Natural Science Foundation of China (41801093 and 41671358), the Provincial Natural Science Foundation of Jiangsu of China (BK20160049), the NIGLAS Cross-functional Innovation Teams (NIGLAS2016TD01), the Youth Innovation Promotion Association of CAS (2012238), and the Ministry of Education of China (grant PCSIRT). X. X. is grateful for the financial support from San Diego State University.

Conflict of Interest

None declared.

Submitted 20 April 2018

Revised 07 August 2018; 16 October 2018; 12 November 2018

Accepted 15 November 2018

Associate editor: Maren Voss